

# Phases of matrix-product states with symmetries and measurements: Finite nilpotent groups

David Gunn<sup>1,2,3</sup>, Georgios Styliaris<sup>4,2</sup>, Barbara Kraus<sup>1,2</sup>, and Tristan Kraft<sup>1,2</sup>

<sup>1</sup>TUM School of Natural Sciences, Technical University of Munich, James-Franck-Str. 1, D-85748 Garching, Germany

<sup>2</sup>Munich Center for Quantum Science and Technology (MCQST), Schellingstr. 4, 80799 München, Germany

<sup>3</sup>International Iberian Nanotechnology Laboratory (INL), Av. Mestre José Veiga, 4715-330 Braga, Portugal

<sup>4</sup>Max Planck Institute of Quantum Optics, Hans-Kopfermann-Str. 1, Garching 85748, Germany

We classify phases of one-dimensional matrix-product states (MPS) under symmetric circuits augmented with symmetric measurements and feedforward. Building on the framework introduced in Gunn *et al.*, Phys. Rev. B 111, 115110 (2025), we extend the analysis from abelian and class-2 nilpotent groups to *all* finite nilpotent groups. For any such symmetry group  $G$ , we construct explicit protocols composed of  $G$ -symmetric circuits and measurements with feedforward that transform symmetry-protected topological (SPT) states into the trivial phase and vice versa using a finite number of measurement rounds determined by the nilpotency class of  $G$ . Although these transformations are approximate, we prove that their success probability converges to unity in the thermodynamic limit, establishing asymptotically deterministic equivalence. Consequently, all SPT phases protected by finite nilpotent groups collapse to a single phase once symmetric measurements and feedforward are allowed. We further show that the same holds for non-normal MPS with long-range correlations, including GHZ-type states. The central technical ingredient is a hierarchical structure of irreducible representations of nilpotent groups, which enables a recursive reduction of non-abelian components to abelian ones. Our results demonstrate that symmetric measurements lead to a complete collapse of both symmetry-protected and non-normal MPS phases for all finite nilpotent symmetry groups.

## 1 Introduction

The classification of quantum phases of matter is a central problem in many-body physics. As in many areas of theoretical physics and mathematics, symmetries serve as a fundamental organizing principle. For the case of gapped phases in one spatial dimension, this perspective has led to a rich structure of phases beyond the traditional Landau paradigm, such as

symmetry-protected topological (SPT) phases. These phases can be systematically classified within the framework of tensor networks, particularly matrix-product states (MPS) [1]. Within this formalism, it is well-established that the phases of MPS protected by global on-site symmetries correspond to elements of the second cohomology group of the symmetry group with coefficients in  $U(1)$  [2, 3]. This classification reflects the interplay between the symmetry group and the structure of the tensors that define the MPS.

An alternative yet equivalent perspective on phases has emerged, based on the action of quantum circuits. In this formalism, two translation-invariant MPS (parameterized by system size  $N$ ) are said to belong to the same phase if there exists a local quantum circuit with depth  $O(\text{polylog } N)$  that maps one to the other [4–7]. When symmetries are present, each gate in the circuit is required to commute with the given representation of the symmetry group. This reformulation has proven powerful in connecting notions of phase equivalence with computational complexity and operationally meaningful transformations.

A practically motivated extension of this framework, inspired by earlier ideas [8–12], is to include, along with quantum circuits, quantum measurements and feedforward [13]. This refers to the case in which unitary gates can be classically conditioned on outcomes of previous measurements in parts of the circuit. This generalized setting is especially natural from the viewpoint of entanglement theory, which is based on the paradigm of local operations and classical communication (LOCC), which includes measurements and feedforward [14]. In this context, a natural question emerges: How does the classification of phases change when measurements and feedforward are allowed, with or without symmetry constraints?

Several results have been obtained in recent years addressing this question without symmetry constraints, particularly for 1D systems [13, 15–18] and for topological phases in 2D [19–25]. In most of these cases, the focus is on how the addition of measurements and feedforward expands the landscape of possible transformations, including experimental implementations [26–28].

When symmetries are imposed, it is essential that the measurements respect the symmetry—not just the unitary gates. To this end, a consistent symmetry-respecting framework was introduced in Ref. [29]. Within this setting, denoted as *G-symmetric Circuits with Measurements and Feedforward* (*G*-CMF), all quantum operations are required to be symmetric with respect to a fixed on-site representation of a symmetry group  $G$ . In particular, in Ref. [29] it was shown that: (i) For a finite abelian symmetry group  $G$ , all symmetric normal MPS belong to a single *G*-CMF phase. This is in contrast to the case without measurement and feedforward, where the classification via cohomology classes in general yields multiple SPT phases. (ii) The same *G*-CMF phase also includes all non-normal (i.e., long-range entangled) MPS, which in the absence of measurements and feedforward, belong to a different phase, even without any symmetry protection. (iii) The *G*-CMF classification for normal MPS also collapses to a single phase for class-2 nilpotent groups, which include all finite abelian groups as a special case but extend beyond them.

Here, we considerably extend these results by providing a systematic classification of *G*-CMF phases for *all* finite nilpotent groups. Nilpotent groups have the special property that the adjoint action,  $\text{ad}_g(h) = [g, h]$ , of any element  $g \in G$ , where  $[g, h] = g^{-1}h^{-1}gh$  denotes the group commutator, terminates in the identity element after a finite number of iterations, i.e.,  $(\text{ad}_g)^M(h) = e$  for all  $h \in G$ . Here,  $M$  is called the nilpotency class of  $G$ , and it is immediate to see that class-1 nilpotent groups are abelian.

We give an explicit *G*-CMF protocol that transforms a distinguished representative of an SPT state to the trivial phase, and vice versa, using finite rounds of measurements, whose number is given by the nilpotency class of  $G$ . Although our transformations are not exact, we prove that they succeed with a probability that approaches one as the system size  $N$  tends to infinity. This thus establishes that all SPT phases of nilpotent groups trivialize with the addition of symmetric measurements. We then consider states with long-range correlations, i.e., non-normal MPS, like the GHZ-type states. Here, we provide a protocol that combines the protocol used to show SPT phases trivialize with fusion measurements and that transforms the trivial phase into non-normal GHZ states. Combined with the reverse transformation, which is similar to the SPT case, this demonstrates that such non-normal phases also trivialize.

As we consider non-abelian groups, the mathematical tools used to derive these results are naturally considerably more involved. At the center of our results is the fact that the irreducible representations of nilpotent groups form a hierarchy (see Secs. 3, and 4, and Ref. [30]). This hierarchy allows us to construct protocols that repeatedly measure and block physical sites, by rules derived from representation theory, in

such a way that after each round of the protocol the resulting state corresponds to lower levels of the hierarchy. These protocols then terminate after finitely many steps in the lowest level of the hierarchy, corresponding to the anticipated target state.

In Section 2 we provide the necessary mathematical background information regarding phases of MPS. In Section 3, we then outline the idea of the protocol that allows us to demonstrate that phases trivialize. In Section 4, we provide more detail as to the mathematical structure of nilpotent groups, including the origin of the finite hierarchy of irreps. Then, in Sections 5 and 6, we prove that SPT and non-normal phases trivialize for all finite nilpotent groups.

## 2 Preliminaries

A tensor,  $A$ , defines a translationally invariant MPS with periodic boundary conditions on  $N$  sites,  $|\psi_N[A]\rangle = \sum_{i_1, \dots, i_N} \text{tr}[A^{i_1} \dots A^{i_N}] |i_1 \dots i_N\rangle$ . Here,  $A^i$  is a  $D \times D$  matrix for all  $i \in \{0, \dots, d-1\}$ , where  $d \in \mathbb{N}$  is the physical dimension and  $D \in \mathbb{N}$  is the *bond dimension*. Mapping the tensor  $A^i$  to the product  $\tilde{A}^{i_1, \dots, i_l} = \prod_{j=1}^l A^{i_j}$  corresponds to “blocking”  $l$  physical sites together into a single supersite. Any MPS tensor, after blocking sufficiently many sites, can be brought into a canonical form,  $A^i = \bigoplus_j A_j^i$ , with the property that the  $A_j^i$  span all matrices with the same block structure [31]. An MPS is called *normal* if, after blocking, its tensor in canonical form has only one block. Given a tensor  $A$ , one may also define its so-called *fiducial state* as

$$|A\rangle = \sum_{i, l, j} (A^i)_{lj} |l\rangle \otimes |i\rangle \otimes |j\rangle, \quad (1)$$

where the system in the middle represents the physical site, whereas systems on the right and left represent virtual sites.

Any MPS tensor in its canonical form can be associated with a parent Hamiltonian for which the MPS is a ground state [3, 32, 33]. Then, two systems are said to be in the same phase if their parent Hamiltonians can be continuously connected by a path of local Hamiltonians without closing the spectral gap above the ground-state subspace in the thermodynamic limit. An alternative yet equivalent definition can be stated in terms of quantum circuits. Here, two MPS belong to the same phase if they can be transformed into one another with “short-depth” local circuits [4]. More precisely, two MPS,  $|\psi_N[A]\rangle$  and  $|\psi_N[B]\rangle$ , belong to the same phase if there exists a sequence of unitaries,  $U_N$ , such that (i)  $\| |\psi_N[A]\rangle - U_N |\psi_N[B]\rangle \|$  converges to 0 as  $N \rightarrow \infty$ , and (ii) each  $U_N$  can be decomposed into a  $O(\text{polylog } N)$ -depth quantum circuit consisting of  $O(1)$ -local nearest neighbor gates. Refs. [2, 3] showed that two MPS belong to the same phase if and only if they have the same number of blocks in canonical form.

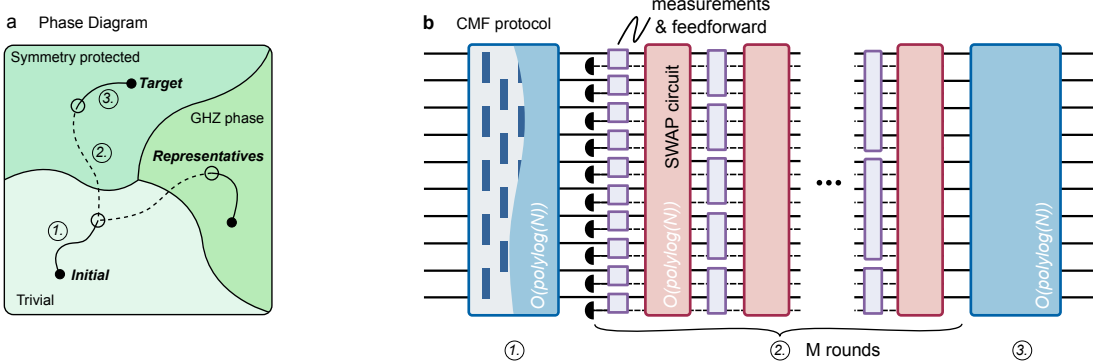


Figure 1: (a) We consider transformations between states belonging to different phases. Starting from an initial state (black dot), for example in the trivial phase, we first transform the state into a phase representative (black circle). This transformation can be implemented by a local symmetric circuit of depth  $O(\text{polylog}(N))$  [4–7]. In the second step, as we will show in detail below, the phase representative is transformed into representatives of other phases using CMF transformations, which include symmetric measurements. In the final step, we again apply a local symmetric circuit of depth  $O(\text{polylog}(N))$  to obtain the desired target state. By constructing explicit protocols that transform between phase representatives, we thereby demonstrate a trivialization of the phase diagram. (b) Circuit representation of a CMF transformation: Blue boxes represent local symmetric unitary circuits corresponding to transformations within phases, i.e., the solid lines in (a). Red boxes represent CMF consisting of multiple rounds of symmetric measurements followed by short-depth symmetric quantum circuits which depend on the measurement outcomes. For class- $M$  nilpotent groups our protocols consist of  $M$  rounds of measurements and circuits. These circuits consist of sequences of nearest-neighbor SWAP gates. While some of our protocols make use of auxiliary systems, other achieve the desired transformation without auxiliary systems.

In addition to the above definition, one can consider systems which are constrained to respect a given symmetry. In this case, new phases of matter emerge: so-called *symmetry protected topological* (SPT) order. In 1D, these phases were characterized in Refs. [2, 3, 34]. In this work, we consider finite global on-site symmetries of the form  $U_g^{\otimes N}$ , where  $U_g$  with  $g \in G$  is some unitary linear representation of a finite group  $G$ , and  $N$  is the number of sites of the system. Then, for a symmetric MPS it holds that  $U_g^{\otimes N} |\psi_N[A]\rangle \propto |\psi_N[A]\rangle$ . The circuits above are then restricted such that each local gate acting on  $n$  sites must commute with the symmetry  $U_g^{\otimes n}$ . The phases are characterized by how the tensor,  $A$ , transforms under the action of the symmetry [2, 3, 34]. In the case of normal MPS, after blocking and bringing it to canonical form, it holds that [3, 35]  $U_g$  is a symmetry iff

$$\sum_j (U_g)_{ij} A^j = e^{i\phi_g} \omega_g^\dagger A^i \omega_g. \quad (2)$$

Here, the phases  $e^{i\phi_g}$  form a 1D unitary irreducible representation (irrep) of  $G$ . The  $\omega_g$  are referred to as *virtual symmetries* and form a *projective representation* of  $G$ , meaning that  $\omega_g \omega_h = \gamma(g, h) \omega_{gh}$ , for all  $g, h \in G$ , where  $\gamma : G \times G \rightarrow U(1)$  is referred to as a *co-cycle*. Crucially, as any transformation  $\omega_g \mapsto \nu(g) \omega_g$  leaves Eq. (3) invariant for  $\nu_g \in U(1)$ , the  $\omega_g$  are only defined up to a phase. Hence  $\gamma(g, h)$  is defined up to the equivalence relation  $\gamma(g, h) \sim \frac{\nu(gh)}{\nu(g)\nu(h)} \gamma(g, h)$ . The induced equivalence classes of the  $\gamma(g, h)$  can be shown to be isomorphic to the second cohomology group of  $G$  over  $U(1)$ ,  $H^2(G, U(1))$ , and thus they are typically referred to as *cohomology classes*

of  $G$ . Throughout, we use  $\mu$  to label the cohomology classes of a given group, with  $\mu = 0$  denoting the trivial class, which corresponds to linear representations. The phase of normal MPS with respect to a given symmetry is specified by the cohomology class of the corresponding projective representation [2, 3, 34]. For non-normal MPS, the phases are specified by a subgroup,  $H \leq G$ , which determines a permutation of the blocks in the canonical form, and by a cohomology class  $\mu \in H^2(H, U(1))$  of  $H$  [2, 3]. That is, phases are specified by the tuple  $(H, \mu)$ , and SPT phases correspond to  $(G, \mu \neq 0)$ . The simplest case of non-normal MPS corresponds to  $(H = 1, \mu = 0)$ , for which we have

$$\sum_j (U_g)_{ij} \left( \bigoplus_k A_k^j \right) = P_g^\dagger \left( \bigoplus_k e^{i\phi_g^k} A_k^i \right) P_g. \quad (3)$$

where  $e^{i\phi_g^k}$  are 1D irreps and the virtual symmetries,  $P_g$ , are permutation representations of the subgroup  $H$  [3] permuting the blocks.

Note that the different phases are labeled by group properties [36], independent of the physical symmetry,  $U_g$ . Nonetheless, for a fixed on-site symmetry, there may be no corresponding symmetric state that belongs to a given phase; see Ref. [29] for an example. To bypass this technicality, we assume throughout this paper that the physical on-site symmetry is given by the regular representation,  $U_g^{\text{reg}} = \sum_{h \in G} |g \circ h\rangle \langle h|$ , where  $\{|h\rangle\}_{h \in G}$  denotes some orthonormal basis and  $\circ$  the group multiplication in  $G$ . The regular representation of a finite group contains all irreducible representations, each appearing with multiplicity equal to its dimension, and has the property that any finite-

dimensional representation of the group appears as a subrepresentation of some tensor power  $(U_g^{\text{reg}})^{\otimes k}$  for sufficiently large but finite  $k$ . Thus, for any desired effective symmetry,  $U_g^{\text{eff}}$ , there is a length-scale, independent of the size of the system, at which the physical symmetry acts as  $U_g^{\text{eff}}$  on a local subspace. As a result, one can show that, with  $U_g^{\text{reg}}$  as the physical on-site symmetry, for every phase,  $(H, \mu)$ , there is a state that belongs to that phase [29].

One can also consider phases of MPS with respect to short-depth circuits and *measurements* [13]. In this framework, one can have  $O(1)$  additional auxiliary systems on-site that can be entangled with the system via the circuits and then measured. In addition, one may perform further circuits after the measurement. In particular, the circuit one performs after a measurement is allowed to depend on the outcome of the measurement (and all previous measurements outcomes). These combined operations are referred to as *circuits, measurements and feedforward* (CMF). In this work, we restrict ourselves to projective measurements, i.e.,  $\{P_i\}_i$  with  $P_i^2 = P_i \geq 0$  and  $\sum_i P_i = 1$ . Naturally, when considering phases with respect to CMF, what is relevant is the cumulative circuit depth of the protocol. Moreover, we consider asymptotically deterministic transformations (i.e., no post-selection); that is, we consider transformations that succeed with a probability that converges to one as  $N \rightarrow \infty$ . Thus, two MPS belong to the same phase with respect to CMF if they can be asymptotically transformed in one another (in the sense of convergent sequences above) via CMF (as described above) with a  $O(\text{polylog}(N))$  cumulative circuit depth. In Ref. [13], it was shown that the inclusion of measurements and feedforward collapses the phase diagram for MPS into a single phase.

As in the case without measurements, one can also consider CMF operations constrained by a symmetry. This is precisely the setting considered in this work. As CMF includes quantum circuits as a subset of its operations, the gates in the circuits are naturally constrained by the symmetry in the same way as before, i.e., each local gate must commute with the symmetry. In addition, one imposes that the measurement operator commute with symmetries, i.e., for each on-site measurement acting on  $n$  sites,  $\{P_i\}_i$ , we must have  $[P_i, U_g^{\otimes n}] = 0$  for all  $i$ . One also imposes that auxiliary systems may be only added and discarded on-site and if they are in a symmetric pure state, unentangled with the rest of the system. Since the discarded and added auxiliary systems need not be the same, one can implement gates that commute up to a phase [29]. We refer to this CMF constrained by symmetries as  $G$ -CMF, where  $G$  refers to a given symmetry group [29]. Note, that  $G$ -CMF without measurements coincides with symmetric circuits, and it coincides with CMF when the symmetry constraints are not imposed (see also Ref. [29] for a more in-depth

discussion). As a result, any phase diagram derived from  $G$ -CMF operations will be a coarse-graining of the standard phase diagram with respect to symmetric circuits and a fine-graining of the phase diagram with respect to CMF.

Under these conditions, we showed in Ref. [29], that the phase diagram of MPS collapses to a single phase for finite *abelian* symmetry groups. This was proven by considering a specific representative of each phase and constructing symmetric CMF transformations between each of these representatives. As symmetric CMF includes symmetric quantum circuits as a subset of its operations, the existence of transformations between these representatives for each phase is sufficient to show that the phase diagram collapses to a single phase, as one may subsequently use symmetric circuits to reach any other point in a phase from its representative. The protocol constructed relied on the ability to perform a symmetric measurement in which all measurement operators were rank-1 projectors. This is demonstrated most clearly in considering transformations to the trivial phase. As a representative for the phase, one may consider a symmetric product state. If one can perform symmetric rank-1 measurements, then clearly one can transform any state, in any phase, to the product state by simply performing symmetric rank-1 measurement on all sites.

For abelian symmetries, such a measurement is possible. In contrast, for non-abelian symmetries, where at least one higher-dimensional irrep exists, the condition  $[P_i, U_g] = 0$  for all  $g \in G$  does not restrict the measurement operators  $P_i$  to rank-1 projectors. In fact, for a symmetry  $U_g$  containing a higher-dimensional irrep, there exists no complete projective measurement consisting only of rank-1 projectors. Thus, a direct transformation to a trivial state though a single round of on-site measurements does not exist in general. However, if a state is locally supported only on invariant subspaces carrying commutative (1D) irreps, then one may, for that given state, deterministically measure outputs corresponding to rank-1 operators. Motivated by this, Ref. [29] showed that phases with respect to the non-abelian dihedral group of eight elements,  $D_8$ —the symmetry group of the square—trivialize under symmetric CMF. Let us recap the key idea.  $D_8$  has five linear irreps. Let us label them  $\{1, 2, 3, 4, 5\}$ , where 1 denotes the trivial representation, 2, 3 and 4 are commutative irreps, and 5 is a non-commutative irrep. Importantly, the tensor product of two copies of the non-commutative irrep decomposes into commutative irreps; namely,  $5 \otimes 5 \cong 1 \oplus 2 \oplus 3 \oplus 4$ . This implies that, after performing local projections onto each irrep  $P_{\alpha \in \{1, 2, 3, 4, 5\}}$ , any outcome that is not rank-1 (specifically, the outcome corresponding to  $P_{\alpha=5}$ ) can be combined with another such outcome to form a composite *supersite* [37]. The resulting supersite has support only on subspaces as

sociated with one-dimensional irreps. Consequently, a subsequent symmetric measurement on this supersite will deterministically yield an outcome corresponding to a rank-1 measurement. In this way, Ref. [29] demonstrated that SPT phases ( $H = G$ ,  $\mu = 1$ ) and the non-normal phase ( $H = 1$ ,  $\mu = 0$ ) of  $D_8$  trivialize. In what follows, we extend these protocols beyond  $D_8$  to all nilpotent groups.

### 3 Outline of the protocol

Here, we outline how the above example can be generalized to all nilpotent groups. To this end, we will recall only those properties of nilpotent groups that are essential for understanding the derivation of the protocols. A more detailed discussion on nilpotent groups and the explicit protocols is provided in the subsequent sections.

Let  $G$  be a nilpotent group, and let  $\text{Irr}$  denote the set of irreps of  $G$ . The irreps of nilpotent groups have the following properties (see Sec. 4 and Ref. [30] for more details):

1. *Hierarchy of irreducible representations:* We can define (see Eq. (10)) a finite hierarchy as a sequence of subsets

$$\text{Irr}_1 \subseteq \text{Irr}_2 \subseteq \dots \subseteq \text{Irr}_M \equiv \text{Irr}, \quad (4)$$

where  $\text{Irr}_1$  denotes the set of all 1D irreps of  $G$ , and  $M$  is the nilpotency class.

2. *Equivalence classes on  $\text{Irr}_m$ :* On each set,  $\text{Irr}_m$ , we can define equivalence classes as follows: For  $\alpha, \beta \in \text{Irr}_m$  we define  $\alpha \sim_m \beta$  if there exists a  $\gamma \in \text{Irr}_{m-1}$  such that the decomposition of  $U_g^\gamma \otimes U_g^\beta$  into irreps contains  $U_g^\alpha$  (see Appendix A for details). In what follows we will then say that  $\alpha$  is contained or appears in  $\gamma \otimes \beta$  or simply  $\alpha \in \gamma \otimes \beta$ .
3. *Group of equivalence classes on level  $m$ :* Crucially, it holds that for each  $m$ , these equivalence classes,  $\text{Irr}_m/\sim = \{[\alpha]_m\}$ , form a group with a group multiplication  $\circ$ , which we define in Sec. 4. This group is isomorphic to a finite abelian group. It has the following properties: The identity element,  $[1]_m \in \text{Irr}_m/\sim$ , corresponds to the irreps in  $\text{Irr}_{m-1}$ . Moreover, the inverse element of  $[\alpha]_m$  is  $[\alpha^*]_m$ , where  $\alpha^*$  is the conjugate representation of  $\alpha$  (see Appendix A). That is,  $[\alpha]_m \circ [\alpha^*]_m = [1]_m = \text{Irr}_{m-1}$ . For any  $\alpha, \beta \in \text{Irr}_m$  we have that  $U_g^\alpha \otimes U_g^\beta$  decomposes only into irreps belonging to  $[\alpha]_m \circ [\beta]_m \in \text{Irr}_m/\sim$ . That is,

$$U_g^\alpha \otimes U_g^\beta = \bigoplus_{\gamma \in \Gamma} U_g^\gamma, \quad \text{with } \Gamma \subseteq [\alpha]_m \circ [\beta]_m. \quad (5)$$

We now consider Hilbert spaces corresponding to a subset of  $n$  sites,  $\mathcal{H}^{\otimes n}$ , and, therefore, representations

of the form  $U_g^{\otimes n}$ . The construction of the protocols relies on the fact that the above structure extends to symmetric projectors, and hence to any symmetry-preserving measurement. Let  $P_\alpha^{(n)}$  be the projector corresponding to, or associated with, the subspace of  $\mathcal{H}^{\otimes n}$  that contains all invariant subspaces of  $U_g^{\otimes n}$  that transform under the irrep  $\alpha$ , i.e. the subspace corresponding to the irrep  $\alpha$  in the decomposition of  $U_g^{\otimes n}$  into irreps. We then collect all projectors corresponding to irreps in the same equivalence class, i.e., we define  $P_{[\alpha]_m}^{(n)} \equiv \sum_{\alpha \in [\alpha]_m} P_\alpha^{(n)}$ . By the property in Eq. (5) above, we have that

$$P_{[\alpha]_m}^{(n)} \otimes P_{[\beta]_m}^{(n')} \subseteq P_{[\alpha]_m \circ [\beta]_m}^{(n+n')}, \quad (6)$$

where  $\subseteq$  indicates that the support on the l.h.s. is contained in the support of the r.h.s. This property will be central for all our protocols.

To see this, consider the case  $m = M$  and suppose we first measure single sites, i.e.,  $n = 1$ . In this case, the set  $\{P_{[\alpha]_M}^{(1)}\}$  forms a complete projective measurement, with outcomes labeled by group elements  $[\alpha]_M \in \text{Irr}_M/\sim$ . Furthermore, suppose that on two neighboring sites we obtain outcomes  $[\alpha]_M$  and  $[\beta]_M$  with  $[\alpha]_M \circ [\beta]_M = [1]_M$ . In this case, the projector  $P_{[\alpha]_M}^{(1)} \otimes P_{[\beta]_M}^{(1)}$  decomposes via Eq. (6) into projectors onto subspaces corresponding exclusively to irreps within  $[1]_M = \text{Irr}_{M-1}$ . Hence, measuring the supersite (in this case composed of two sites), will only lead to outcomes corresponding to group elements in  $\text{Irr}_{M-1}/\sim$ . In the example of  $D_8$ , this corresponds to  $P_{[5]_2}^{(1)} \otimes P_{[5]_2}^{(1)}$ , which decomposes into 1D projectors ( $P_{[5]_2}^{(1)} \otimes P_{[5]_2}^{(1)} \subseteq P_{[1]_2}^{(2)}$ ), as  $5 \otimes 5 \simeq 1 \oplus 2 \oplus 3 \oplus 4$  and  $[1]_2 = \{1, 2, 3, 4\}$ . In general, we will start with the first measurement corresponding to  $\{P_{[\alpha]_M}^{(1)}\}$  (which is a local complete measurement, as  $\text{Irr}_M$  contains all irreps). Then, perform a subsequent measurement on supersites with  $m = M - 1$ . In this case, the set  $\{P_{[\alpha]_{M-1}}^{(n)}\}$  needs to be augmented with an additional (orthogonal) projector to form a complete measurement. However, due to the previous measurement round, this outcome will never occur, and all possible outcomes can be labeled by  $[\alpha]_{M-1} \in \text{Irr}_{M-1}/\sim$ .

Suppose that all measurements in the first round can be grouped so that their product equals the identity element  $[1]_M$ . Then the above argument applies to each such supersite. Therefore, in the second round we obtain exclusively measurement outcomes in  $\text{Irr}_{M-1}/\sim$ . Moreover, this procedure can be repeated and as the hierarchy eventually reaches one-dimensional irreps,  $\text{Irr}_1$ , the process guarantees that after  $M - 1$  rounds the supersites have support only on irreps in  $\text{Irr}_1$ . At this point, we can perform a measurement composed of rank-1 projectors which deterministically transforms the state to a product state in the trivial phase. In Fig. 2, we give an example of such a protocol using the non-abelian group  $D_{16}$  which has

nilpotency class three. The only remaining part is to show that such a protocol uses only  $O(\text{polylog}(N))$  circuit depth.

To this end, we note that the overall measurement outcomes in each round multiply to the identity. This is guaranteed by the fact that we perform a measurement on all sites of a pure symmetric state (the initial state and the state after the  $m$ -th round). A pure symmetric state belongs to the invariant subspace of  $U_g^{\otimes N}$  that corresponds to a 1D irrep  $\alpha \in \text{Irr}_1$  and  $\text{Irr}_1 \subseteq [1]_m$  for all  $m \in \{2, \dots, M\}$ . Therefore, the product of all measurement outcomes of symmetric measurements performed on such a state always equals the identity, i.e.,  $\circ_i[\alpha_i]_m = [1]_m$ .

This ensures that the measurement outcomes can be partitioned into subsets that also multiply to the identity. Thus, it only remains to show that those partitions are sized  $O(\log(n))$  and that the reordering of the sites according to this partition can be performed via a  $O(\text{polylog}(N))$  depth circuit. As we will show in the next section, one can construct transformations such that the probability of encountering cases that require permutation circuits of depth exceeding  $O(\text{polylog}(N))$  vanishes in the thermodynamic limit  $N \rightarrow \infty$ .

We will show that a protocol of the above form directly leads to the trivialization of all SPT phases—the protocol transforms SPT states to separable states in the trivial phase. Note that this also implies the reverse direction as two copies of an SPT phase also belong to the trivial phase [3]. Moreover, we will show that similar, but slightly more sophisticated protocols also lead to a trivialization of the non-normal phases.

## 4 Finite nilpotent groups and their representations

As a preparation for the following discussion, we need to recall some known facts about nilpotent groups and their (irreducible) representations [38, 39]. Let  $G$  be a finite group. The group commutator is defined by  $[g, h] = g^{-1}h^{-1}gh$  for all  $g, h \in G$ . The commutator subgroup, denoted by  $[G, G]$ , is the subgroup generated by all elements of the form  $[g, h]$ , with  $g, h \in G$ . The *lower central series*,

$$G \equiv G_0 \trianglerighteq G_1 \trianglerighteq G_2 \trianglerighteq \dots, \quad (7)$$

where  $\trianglerighteq$  indicates a normal subgroup, is a descending series of subgroups that is obtained by repeatedly taking commutator subgroups of  $G$ , i.e.,  $G_0 \equiv G$  and  $G_{m+1} = [G_m, G]$  for  $m \geq 0$ . The crucial property of nilpotent groups is that there exists an  $M \in \mathbb{N}$  at which the lower central series terminates in the trivial group. That is,

$$G = G_0 \trianglerighteq G_1 \trianglerighteq \dots \trianglerighteq G_M = \{e\}. \quad (8)$$

A nilpotent group is *class- $M$  nilpotent* if  $M$  is the smallest such integer. Abelian groups are class-one nilpotent.

Using the lower central series of a class- $M$  nilpotent group  $G$ , we define the following sequence of subsets of the set of irreducible representations of  $G$ :

$$\{1\} \equiv \text{Irr}_0 \subseteq \text{Irr}_1 \subseteq \dots \subseteq \text{Irr}_M \equiv \text{Irr}, \quad (9)$$

where  $\text{Irr}_m$  is the set of all irreps of  $G$  for which the representation matrix of any element in  $G_m$  equals the identity, i.e.,

$$\text{Irr}_m \equiv \{\alpha \in \text{Irr} : U_g^\alpha = \mathbf{1}_{d^\alpha}, \forall g \in G_m\}, \quad (10)$$

with  $m \in \{0, \dots, M\}$  and  $d^\alpha$  the dimension of the irrep. For instance, we have that  $\text{Irr}_0$  contains only the trivial representation,  $\text{Irr}_1$  contains all 1D irreps of  $G$ , and  $\text{Irr}_M$  contains all irreps of  $G$ . Note that due to Eq. (10) we have that all irreps occurring in  $\alpha \otimes \beta$  belong to  $\text{Irr}_m$  for any  $\alpha, \beta \in \text{Irr}_m$ .

We will now define an equivalence relation for each of the sets  $\text{Irr}_m$ . It is based on the properties of tensor product of irreps of nilpotent groups (see also Ref. [30]). Two irreps  $\alpha, \beta \in \text{Irr}_m$  are said to be equivalent if there exists an irrep one step below in the hierarchy,  $\gamma \in \text{Irr}_{m-1}$ , such that  $\alpha$  appears in the decomposition of  $\gamma \otimes \beta$ . That is,

$$\beta \sim_m \alpha \text{ if } \exists \gamma \in \text{Irr}_{m-1} : \alpha \in \gamma \otimes \beta, \quad (11)$$

where by  $\alpha \in \gamma \otimes \beta$  we mean that the irrep  $\alpha$  appears in the decomposition into irreps of the representation corresponding to the tensor product of the irreps  $\gamma$  and  $\beta$ . It is verified in Appendix A that this is indeed an equivalence relation. We denote the equivalence class of  $\alpha$  under  $\sim_m$  by  $[\alpha]_m$ , and we drop the subscript  $m$  whenever it is clear from context.

Now, let us also introduce a group multiplication,  $\circ$ , on  $\text{Irr}_m/\sim$  by defining  $[\alpha] \circ [\beta]$  as those irreps that appear in the decomposition into irreps of  $\alpha' \otimes \beta'$  for all  $\alpha' \sim \alpha$  and  $\beta' \sim \beta$ . That is,

$$[\alpha] \circ [\beta] = \{\delta \in \text{Irr}_m : \exists \alpha' \in [\alpha], \beta' \in [\beta] : \delta \in \alpha' \otimes \beta'\}. \quad (12)$$

In Appendix A, we show that  $(\text{Irr}_m/\sim, \circ)$  does indeed form a group, and moreover, that this group is isomorphic to the abelian quotient group

$$G_{m-1}/G_m \simeq \text{Irr}_m/\sim. \quad (13)$$

Furthermore, in Appendix B, we provide an example of a nilpotent group and explain its properties regarding the structures discussed above.

The identity element of  $\text{Irr}_m/\sim$ ,  $[1]_m \in \text{Irr}_m/\sim$ , is the equivalence class containing all irreps from one level below in the hierarchy, i.e.,  $[1]_m = \text{Irr}_{m-1}$ . Moreover, for any  $\alpha \in \text{Irr}_m$ , its conjugate representation,  $\alpha^*$ , belongs to the group inverse in  $(\text{Irr}_m/\sim, \circ)$ , i.e.,  $\alpha^* \in [\alpha]^{-1}$ , as the tensor product of  $\alpha$  and  $\alpha^*$  decomposes into irreps belonging to  $\text{Irr}_{m-1}$  (see Appendix A).

The group structure of the equivalence classes in Eq. (12) allow us to constrain the specific irreps that occur in the decomposition of  $\alpha \otimes \beta$ . Specifically, one finds that

$$U_g^\alpha \otimes U_g^\beta = \bigoplus_{\gamma \in \Gamma \subseteq [\alpha] \circ [\beta]} U_g^\gamma, \quad (14)$$

where every irrep  $\gamma$  appearing in the decomposition of  $\alpha \otimes \beta$  lies in the equivalence class  $[\alpha] \circ [\beta]$ , although not all such irreps necessarily occur. These will be the key properties that we will use to derive protocols which transform states of one phase into another phase.

To this end, throughout the paper, we will repeatedly use projective measurements, where the projectors project onto subspaces associated with the equivalence classes in  $\text{Irr}_m$ . We will write  $\{P_{[\alpha]}^{(n)}\}_{[\alpha] \in \text{Irr}_m}$  to represent the projection onto the subspaces of  $U_g^{\otimes n}$  associated with irreps in  $[\alpha]$ ; that is (see Ref. [40], Theorem 8),

$$P_{[\alpha]}^{(n)} = \sum_{\alpha \in [\alpha]} P_\alpha^{(n)} = \sum_{\alpha \in [\alpha]} \sum_{g \in G} \frac{d^\alpha \bar{\chi}_g^\alpha}{|G|} U_g^{\otimes n}, \quad (15)$$

with  $P_\alpha^{(n)}$  the projector onto the subspace associated with  $\alpha \in \text{Irr}$  in  $U_g^{\otimes n}$ . Note that due to Eq. (14), we have that

$$P_{[\alpha]}^{(n)} \otimes P_{[\beta]}^{(n')} \subseteq P_{[\alpha] \circ [\beta]}^{(n+n')}, \quad (16)$$

where  $\subseteq$  indicates the support on the l.h.s. is contained in the support of the r.h.s. This property will be used repeatedly throughout this work as it implies that if we measure  $n$  sites and get outcomes corresponding to local measurements  $P_{[\alpha_i]}$  with  $[\alpha_i] \in \text{Irr}_m / \sim$  such that  $\circ[\alpha_i] = [1] \in \text{Irr}_m / \sim = \text{Irr}_{m-1}$ , then we can combine these  $n$  sites and measure (the complete measurement given by)  $\{P_{[\beta]}^{(n)}\}_{[\beta] \in \text{Irr}_{m-1} / \sim}$  together with some additional orthogonal projector, which will never be measured, as we will see. In this way, in each round,  $m$ , we can deterministically projected onto subspaces corresponding to irreps in  $\text{Irr}_{m-1}$ , until we are projecting onto subspaces corresponding to irreps in  $\text{Irr}_1$  (i.e., the abelian subspace).

In the following, we will evaluate equations that involve Eq. (15). The following technical lemma simplifies those calculations by providing a more compact expression for the above projectors. The proof of this lemma can be found in Appendix C.

**Lemma 1.** *Let  $\text{Irr}_m / \sim \cong G_{m-1} / G_m = \{[\alpha]\}$ . Then, we have the following:*

$$P_{[\alpha]}^{(n)} = \sum_{g \in G_{m-1}} \frac{e^{-i\varphi^{[\alpha]}([g])}}{|G_{m-1}|} U_g^{\otimes n}, \quad (17)$$

where  $[g]$  denotes the canonical projection map from  $G_{m-1}$  to  $G_{m-1} / G_m$ , and  $e^{-i\varphi^{[\alpha]}} \in \text{Irr}(G_{m-1} / G_m)$  is a 1D irrep of  $G_{m-1} / G_m$  defined in Appendix C.

## 5 Trivialization of symmetry-protected phases

In this section, we show the trivialization of symmetry-protected phases. We describe a protocol that transforms an SPT state into a product state in the trivial phase while respecting the symmetry described by a finite nilpotent group. The protocol proceeds in  $M$  rounds of measurements interleaved with low-depth circuits. The reverse transformation then follows immediately as two copies of an SPT state belong to the trivial phase [3]; transforming one copy to the trivial phase leaves an SPT state on the second.

We begin by choosing a representative state for the SPT phase. We then explain the details of our protocol and demonstrate that it successfully achieves the desired transformation. Then, we analyze the resources required for its implementation, including its circuit depth and probability of success.

### 5.1 Representative for the phase

Let  $G$  be a class- $M$  nilpotent group with a non-trivial second cohomology group  $H^2(G, U(1))$ . Associated with each  $\mu \in H^2(G, U(1))$  is a cocycle  $\gamma^\mu : G \times G \rightarrow U(1)$ , and the so-called *projective  $\mu$ -regular representation* is given by [41]

$$\omega_g^\mu = \sum_{h \in G} \gamma_{g,h}^\mu |g \circ h\rangle\langle h|. \quad (18)$$

As before,  $\{|h\rangle\}_{h \in G}$  denotes some orthonormal basis and  $\circ$  the group multiplication in  $G$ . This generalizes the linear regular representation of a group  $G$ , and if  $\mu$  is trivial the projective  $\mu$ -regular representation reduces to the linear regular representation of  $G$ . This representation is reminiscent of the generalized Pauli matrices, sometimes also referred to as clock- and shift matrices. Indeed, they fulfill similar properties as the generalized Paulis. For instance, they are mutually orthogonal under the Hilbert-Schmidt inner product, i.e.,

$$\text{tr}(\omega_g^{\mu\dagger} \omega_h^\mu) = |G| \delta_{g,h}, \quad (19)$$

for all  $g, h \in G$ , and, as projective representations, they are closed under multiplication up to phases, i.e.,  $\omega_g^\mu \omega_h^\mu = \gamma_{gh}^\mu \omega_{gh}^\mu$ . Fix a non-trivial  $\mu$  and define the effective on-site symmetry

$$U_g = (\omega_g^\mu)^* \otimes \omega_g^\mu. \quad (20)$$

As we consider the on-site symmetry to be the regular representation, there is a finite blocking length,  $k$ , at which the above effective on-site symmetry appears as a subrepresentation of  $(U_g^{\text{reg}})^{\otimes k}$  (see Section 2). Then, a representative for the SPT phase can be chosen as [2, 3]

$$|\text{SPT}\rangle = \bigotimes_{i=1}^N |\Phi_{|G|}^+\rangle_{i,i+1}, \quad (21)$$

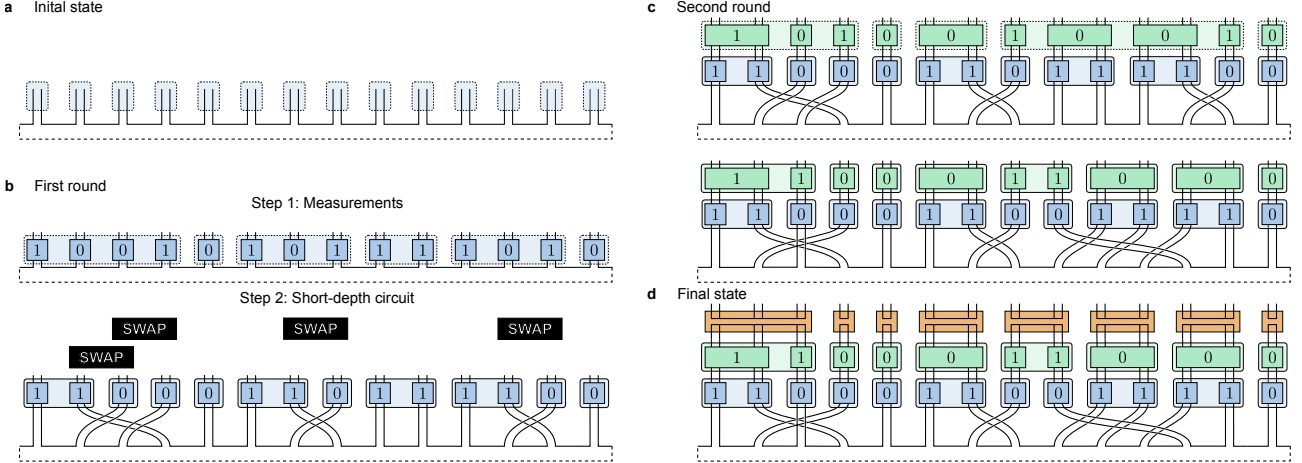


Figure 2: An example of the SPT protocol for the non-abelian class-3 nilpotent group  $D_{16}$ , transforming an SPT state to the trivial phase. (a) We depict the initial non-trivial state,  $|\text{SPT}\rangle$ , corresponding to a chain of Bell pairs between nearest neighbors. This state is symmetric under  $U_g^{\otimes N}$ , with the effective symmetry defined in Eq. (20). (b) In the first round of the protocol, we project onto the equivalence classes in  $\text{Irr}_3/\sim$ , with projectors represented by blue boxes. Due to the isomorphism in Eq. (13) we have that  $\text{Irr}_3/\sim \cong G_2/G_3 \cong \mathbb{Z}_2$ . Therefore, measurement outcomes can be labeled by elements of  $\mathbb{Z}_2$ . Note, that the total product of outcomes is equal to 0, the identity element. Next, we partition the output into minimal connected substrings that multiply to the identity. Here, the longest minimal connected substring that multiplies to the identity is of length 4. Therefore, we need  $L^{(1)} \geq 16$  to ensure the protocol does not fail in this step. In a second step we use a SWAP circuit to permute these minimal connected substrings to get substrings of length at most  $|G_2|/|G_3| = 2$  that multiply to the identity. This is to ensure that subsequent measurements act on only  $O(1)$  sites. By inspection, we see that the second round will measure  $N^{(2)} = 10$  supersites. (c) In the second round of the protocol, we then project onto the equivalence classes in  $\text{Irr}_2/\sim$ , with projectors represented by green boxes. Outcomes are labeled by  $\text{Irr}_2/\sim \cong G_1/G_2 \cong \mathbb{Z}_2$ . As before, we use a circuit to permute the outcome. Then, substrings have support on subspace of 1D irreps. Finally, in (d), we project onto 1D subspaces, represented by orange boxes. As these measurements are rank-1, the resulting state is a symmetric pure product state with local sites of size  $O(|G|)$ .

which is a chain of maximally-entangled Bell states between nearest neighbors, see Fig. 2(a). This will be our representative state for the SPT phases. Next, we will show how to transform this state to a product state in the trivial phase.

## 5.2 Protocol

Having fixed representatives of the phases, we now present a protocol that maps the state  $|\text{SPT}\rangle$  in Eq. (21) to a separable state in the trivial phase. We will explain the first round in more detail, and briefly comment on subsequent rounds, which then proceed similarly. In Fig. 2 we provide an example that illustrates the following protocol.

### 5.2.1 First round

On each site, we perform the projective measurement  $\{P_{[\alpha]}^{(1)}\}$ , where  $P_{[\alpha]}^{(1)}$ , as defined in Eq. (15), projects onto the subspace associated with those irreps in  $U_g$  that belong to  $[\alpha] \in \text{Irr}_M/\sim$ . We can label the measurement outcome by a vector

$$\mathbf{x}^{(1)} = (x_1^{(1)}, x_2^{(1)}, \dots, x_N^{(1)}), \quad (22)$$

where  $x_i^{(1)} \in \text{Irr}_M/\sim$ , and  $N \equiv N^{(1)}$  is the number of sites with the upper index referring to the measurement round.

On the level of the entire system of  $N$  sites, the outcomes are correlated. The only outcomes to occur are those where  $x_1^{(1)} \circ \dots \circ x_N^{(1)} = [1] \in \text{Irr}_M/\sim$ . As mentioned before, the reason for that is that the global state is pure and symmetric and thus must belong to the abelian subspace, i.e., the subspace of  $U_g^{\otimes N}$  associated with irreps in  $\text{Irr}_1$ . As  $\text{Irr}_1 \subseteq [1] \in \text{Irr}_M/\sim$  we have that [42]

$$\begin{aligned} x_1^{(1)} \circ \dots \circ x_N^{(1)} &\neq [1] \\ \Rightarrow \langle \text{SPT} | P_{x_1^{(1)}} \otimes \dots \otimes P_{x_N^{(1)}} | \text{SPT} \rangle &= 0. \end{aligned} \quad (23)$$

After the first round of measurements, we can partition the outcome vector  $\mathbf{x}^{(1)}$  into the shortest connected substrings that individually multiply to the identity element, see Fig. 2(b) for an example. If the longest of such substrings is greater than  $L^{(1)}$ , where  $L^{(1)}$  is some yet to be specified function of  $N^{(1)} = N$ , the protocol terminates and fails. Later we will show that if we choose  $L^{(1)} = O(\log(N))$  with a sufficiently large constant prefactor, then the probability that there is a substring longer than  $L^{(1)}$  vanishes in the thermodynamic limit.

Assuming that the longest of such substrings is not greater than  $L^{(1)}$ , we use a SWAP circuit to permute each substring in such a way that one obtains minimal connected substrings that each multiply to identity and are of length at most  $|G_{M-1}|/|G_M|$  (see Fig. 2(c))

for an example). This follows from the fact that  $|G_{M-1}|/|G_M|$  is finite. By doing so, we have transformed our vector of outcomes  $\mathbf{x}^{(1)} \mapsto \tilde{\mathbf{x}}^{(1)}$ , where the latter can be partitioned as

$$\tilde{\mathbf{x}}^{(1)} = (\tilde{x}_i^{(1)})_{i=1}^{N^{(2)}}, \quad (24)$$

where  $N^{(2)} = N^{(2)}(\mathbf{x}^{(1)})$  is the number of such substrings, which depends on  $\mathbf{x}^{(1)}$ . As all substrings,  $\tilde{x}_i^{(1)}$ , multiply to the identity element  $[1]_M$ , the sites associated with each  $\tilde{x}_i^{(1)}$  are supported only on subspaces associated with irreps in  $\text{Irr}_{M-1} = [1]_M$ . Therefore, in the next round, we will project onto subspaces associated with irreps in  $\text{Irr}_{M-1}$ .

### 5.2.2 Second round

In the second round, we consider the system on a scale of the substrings defined in the first round. On the sites corresponding to each substring, we perform the measurement  $\{P_{[\beta]}^{(N_i^{(1)})}\}$  where  $N_i^{(1)} \leq |G_{m-1}|/|G_m|$  is the length of the  $i^{th}$  substring from round one and  $[\beta] \in \text{Irr}_{M-1}/\sim$ . As the projective measurements in the different rounds commute, we again obtain a parity constraint,  $[\beta_1] \circ \dots \circ [\beta_{N^{(2)}}] = [1] \in \text{Irr}_{M-1}$ . We then proceed as in the first round.

### 5.2.3 Subsequent rounds

We proceed as in previous rounds. After  $M-1$  measurements and subsequent circuits, we will have obtained sites all locally supported on irreps belonging to  $\text{Irr}_1/\sim = \text{Irr}_1$  which contains all 1D irreps. Thus, the state is locally supported on a subspace that decomposes into 1D irreps. Therefore, in a final measurement, we can disentangle the state and locally correct the outcome to obtain a translation invariant state in the trivial phase.

## 5.3 Resources

Now let us study the resources required for the protocol. A round begins when a measurement is made and ends after any subsequent circuits. In round  $m \in \{1, \dots, M\}$ , we project onto the different subspaces associated with equivalence classes of irreps in  $\text{Irr}_{M-(m-1)}/\sim \cong G_{M-m}/G_{M-(m-1)}$ . After permuting outcomes and forming minimal connected substrings that multiply to the identity element the supersites consist of at most  $|G_{M-m}|/|G_{M-(m-1)}|$  supersites from the previous round. Thus, after  $k$  rounds, the supersites consist of at most  $\prod_{m=1}^k |G_{M-m}|/|G_{M-(m-1)}| = |G_{M-k}|/|G_M| = |G_{M-k}|$  original sites, where the last equality follows from  $G_M = \{e\}$ , and therefore, the size of measured sites is independent of system-size. Moreover, as the number of rounds is finite, at the end of the protocol supersites are of size  $O(|G|)$ .

Next, let us consider the cumulative circuit depth of the protocol. In round  $m$ , we perform permutations on substrings of length at most  $L^{(m)}$ . Recall, that if the longest minimal connected substring whose product is the identity has length greater than  $L^{(m)}$ , the protocol terminates and fails. An arbitrary permutation of  $n$  sites can be performed using a SWAP circuit of depth at most  $4n$  [43]. Thus, the SWAP circuit in round  $m$  has depth at most  $O(L^{(m)}(N^{(m)}))$  at the length-scale of round  $m$ . We note again, that each round effectively rescales the length-scale at which we operate. Moreover,  $N^{(m)} \leq N$ . Therefore, we may upper bound the cumulative circuit depth of the protocol with  $\max_m O(|G_m|L^m(N))$ . In the subsequent sections, we will show that choosing  $L^{(m)}(n) = O(\log(n))$ , with a sufficiently large constant prefactor, is sufficient to ensure the probability of success converges to 1 as  $N \rightarrow \infty$ . For such a choice, the cumulative circuit depth is  $O(\log(N))$ .

## 5.4 Probability distribution of measurement outcomes

In this section, we show that the outcome distribution in every round is uniform, subject to a parity constraint. It suffices to analyze the second round of measurement, since all other rounds follow analogously.

The probability distribution of the outcome of the second round,  $\mathbf{x}^{(2)}$ , depends on the outcome in the first round,  $\mathbf{x}^{(1)}$ . Indeed, the number of supersites measured in a given round depends on the measurement outcome of the preceding round. Recall that, given an outcome  $\mathbf{x}^{(1)}$  in the first round, we permute it to obtain  $\tilde{\mathbf{x}}^{(1)}$ . The string  $\tilde{\mathbf{x}}^{(1)}$  then decomposes into  $N^{(2)}$  substrings of length at most  $|G_{M-1}|/|G_M|$  that individually multiply to the identity.

For simplicity, let us consider the case where no permutation is needed (we will consider the case with permutations between measurements at the end). In this case, we can partition  $\mathbf{x}^{(2)}$  and  $\mathbf{x}^{(1)}$  using the same indices. Thus we can write

$$\begin{aligned} \mathbf{x}^{(2)} &= (\mathbf{x}_i^{(2)})_{i=1}^{N^{(2)}}, \\ \mathbf{x}^{(1)} &= (\mathbf{x}_i^{(1)})_{i=1}^{N^{(2)}} = ((x_{ij}^{(1)})_{j=1}^{N_i^{(1)}})_{i=1}^{N^{(2)}}. \end{aligned} \quad (25)$$

Note that, since the outcome in the first round satisfied a parity constraint (see Eq. (23)) and required no rearrangement,

$$\prod_j x_{ij}^{(1)} = [1], \quad \forall i. \quad (26)$$

Then, we can express the conditional probability of observing  $\mathbf{x}^{(2)}$  in the second round, given that we have

observed  $\mathbf{x}^{(1)}$  in the first round, as

$$\begin{aligned}
p(\mathbf{x}^{(2)}|\mathbf{x}^{(1)}) &= \frac{\text{tr} \left( \begin{array}{c} \text{blue boxes} \\ \text{green boxes} \end{array} \right)}{\text{tr} \left( \begin{array}{c} \text{blue boxes} \\ \text{green boxes} \end{array} \right)} \\
&= \frac{\text{tr} \left( \begin{array}{c} \text{blue boxes} \\ \text{green boxes} \end{array} \right)}{\text{tr} \left( \begin{array}{c} \text{blue boxes} \\ \text{green boxes} \end{array} \right)} \quad (27)
\end{aligned}$$

where the blue boxes correspond to projectors onto subspaces associated with equivalence classes in  $\text{Irr}_{M-1}/\sim$  and the green boxes correspond to projectors onto subspaces associated with equivalence classes  $\text{Irr}_{M-2}$  (see Fig. 2 for comparison). The second equality follows from the cyclic property of the trace and the fact that

$$[P_{x_i^{(2)}}, \bigotimes_j P_{x_{ij}^{(1)}}] = 0, \quad \forall i \quad (28)$$

due to Eq. (26). To evaluate the conditional probability, consider the first term in the numerator

$$\begin{array}{c} x_1^{(2)} \\ \text{---} \\ x_{11}^{(1)} x_{i2}^{(1)} \end{array} \quad (29)$$

Using Lemma 1 and the fact that  $U_g = \omega_g^* \otimes \omega_g$ , this evaluates to

$$\begin{aligned}
&\sum_{\substack{b_1 \in G_{M-2} \\ a_{11}, a_{12} \in G_{M-1}}} \frac{e^{-i\phi^{x_i^{(2)}}([b_1])}}{|G_{M-2}|} \frac{e^{-i\phi^{\tilde{x}_{ij}^{(1)}}([a_{i1}])}}{|G_{M-1}|} \frac{e^{-i\phi^{\tilde{x}_{ij}^{(1)}}([a_{i1}])}}{|G_{M-1}|} \\
&\times \begin{array}{c} \text{---} \\ \omega_{b_1}^* \quad \omega_{b_1} \quad \omega_{b_1}^* \quad \omega_{b_1} \\ | \quad | \quad | \quad | \\ \omega_{a_{11}}^* \quad \omega_{a_{11}} \quad \omega_{a_{12}}^* \quad \omega_{a_{12}} \end{array} \quad (30)
\end{aligned}$$

Consider the loop in this equation. Each factor  $\omega_{b_i} \omega_{a_{ij}}$  appears together with its conjugate in  $U_g$ , so the phases arising from the multiplication of projective representations cancel. Moreover, the projective  $\mu$ -regular representations are orthogonal by Eq. (19). Consequently, these loops yield delta functions of the form

$$|G| \delta(b_i a_{ij} = b_{(ij \oplus 1)} a_{ij \oplus 1}), \quad (31)$$

where  $(ij \oplus 1)$  denotes the next index in the chain.

Now we consider that for each substring of  $\mathbf{x}^{(1)}$ , we have

$$b_i a_{ij} = b_i a_{ij'} \Rightarrow a_{ij} = a_{i1} \Rightarrow [a_{ij}] = [a_{i1}], \quad (32)$$

for all  $i, j$ , where  $[\cdot]$  denotes the canonical projection from  $G_{M-1} \rightarrow G_{M-1}/G_M$ . Moreover, if we consider the boundaries between substrings, we get that for all  $i$

$$b_i a_{iN_i^{(1)}} = b_{i \oplus 1} a_{i \oplus 1, 1} \Rightarrow [b_i] = [b_1], \quad (33)$$

where  $[\cdot]$  denotes the canonical projection from  $G_{M-2} \rightarrow G_{M-2}/G_{M-1}$ . Thus, the numerator of Eq. (27) becomes

$$|G|^N \sum_{\substack{b_1 \in G_{M-2} \\ a_{i1} \in G_{M-1}}} \left( \prod_{i=1}^{N^{(2)}} \frac{e^{-i\phi^{x_i^{(2)}}([b_1])}}{|G_{M-2}|} \prod_{j=1}^{N_i^{(1)}} \frac{e^{-i\phi^{\tilde{x}_{ij}^{(1)}}([a_{i1}])}}{|G_{M-1}|} \right). \quad (34)$$

Using the fact that the phases are 1D irreps, and Eq. (26) this evaluates to

$$|G|^N \left( \frac{|G_M|}{|G_{M-1}|} \right)^{N-1} \left( \frac{|G_{M-1}|}{|G_{M-2}|} \right)^{N^{(2)}-1} \delta \left( \prod_i x_i^{(2)} = [1] \right). \quad (35)$$

It is easily seen through the same arguments that the denominator of Eq. (27) evaluates to the first term in the equation above. Thus

$$p(\mathbf{x}^{(2)}|\mathbf{x}^{(1)}) = \left( \frac{|G_{M-1}|}{|G_{M-2}|} \right)^{N^{(2)}-1} \delta \left( \prod_i x_i^{(2)} = [1] \right), \quad (36)$$

and therefore,  $p(\mathbf{x}^{(2)}|\mathbf{x}^{(1)})$  is uniform with a parity constraint.

Let us consider the effect of a permutation circuit between measurement one and two. In this case, the delta function in Eq. (31) becomes

$$\delta(b_{(ij)} a_{ij} = b_{(\sigma(ij \oplus 1) \oplus 1)} a_{\sigma(ij \oplus 1)}), \quad (37)$$

where  $\sigma$  is the permutation applied to the sites. However, as  $\sigma$  is a bijection, all delta functions can be rearranged to obtain the original conditions. Thus the permutations have no effect on the probability. Finally, it is clear how the above arguments extend to all other rounds. Thus, the above arguments demonstrate that the probability distribution of outputs in every round of the protocol is uniform with a parity constraint.

## 5.5 Probability of success

We now show that, when we restrict ourselves to circuits of depth  $O(\log(N))$ , the probability of success converges to one as  $N \rightarrow \infty$ . Therefore, let us analyze the probability of failure in each given round.

### 5.5.1 First round

A necessary condition for the protocol to fail in the first round is that there exists at least one connected substring  $\mathbf{y}$  of length  $L^{(1)}$  in  $\mathbf{x}^{(1)}$  whose elements do not multiply to the identity, i.e.,

$$y_1 \circ \cdots \circ y_{d'} \neq [1] \in G_{M-1}/G_M, \quad \forall d' = 1, \dots, L^{(1)}. \quad (38)$$

In the following, we refer to such strings as “ $L^{(1)}$  substrings”. This condition is not sufficient: such a substring may appear without causing failure due to the periodic boundary condition [44].

As the above condition is necessary, the probability of the protocol failing in the first round is upper bounded by the probability of obtaining such a substring. Moreover, we can derive a loose upper bound on the probability of observing such a substring by summing, over all starting positions  $j$ , the probabilities of all strings that contain an  $L^{(1)}$ -substring beginning at position  $j$ .

Consider an  $L^{(1)}$ -substring beginning at position  $j$ . If the measurements were performed sequentially, obtaining an  $L^{(1)}$ -substring would correspond to each subsequent measurement not being the inverse of the product of the previous measurements (see Eq. (38)). Since the probability distribution is uniform up to a global constraint, the inverse would occur in each subsequent measurement with probability  $1/(|G_{M-1}|/|G_M|)$  (except for the last measurement, which would be fixed by the parity constraint). Therefore, the probability of an outcome containing an  $L^{(1)}$ -substring beginning at position  $j$  is upper bounded by  $(1 - |G_M|/|G_{M-1}|)^{L^{(1)}}$ , cf. Ref. [45]. This argument applies to each starting position  $j$ , and thus

$$p_{\text{fail}}^{(1)} \leq N \left( 1 - \frac{|G_M|}{|G_{M-1}|} \right)^{L^{(1)}}. \quad (39)$$

Therefore, if we choose

$$L^{(1)} = C_1 \log(N), \quad (40)$$

with  $C_1 = \frac{-(1+R_1)}{\log \left( 1 - \frac{|G_M|}{|G_{M-1}|} \right)}$  for any  $R_1 > 0$ , then

$$p_{\text{fail}}^{(1)} \leq \frac{1}{N^{R_1}} \rightarrow 0. \quad (41)$$

### 5.5.2 Second round

If the protocol succeeds in the first round with outcome  $\mathbf{x}^{(1)}$ , then after permuting the sites, the second-round measurement is performed on at least  $N/(|G_{M-1}|/|G_M|) = N/|G_{M-1}|$  sites. The protocol then fails if the measurement outcome contains an  $L^{(2)}$ -substring. The failure probability can be upper bounded as in the first round. Namely, by choosing  $L^{(2)}(N) = C_2 \log(N)$ , with  $C_2 = \frac{-(1+R_2)}{\log \left( 1 - \frac{|G_{M-1}|}{|G_{M-2}|} \right)}$  and

$R_2 > 0$  we have

$$p_{\text{fail}}^{(2)}|_{\mathbf{x}^{(1)}} \leq \left( \frac{|G_{M-1}|}{N} \right)^{R_2}, \quad (42)$$

for all  $\mathbf{x}^{(1)}$ . Therefore, the probability of the protocol failing in the second round is also upper bounded by  $(|G_{M-1}|/N)^{R_2}$ , and, therefore, the probability of having failed in the first *or* second round is bounded by

$$p_{\text{fail}}^{(2)} \leq \frac{1}{N^{R_1}} + |G_{M-1}|^{R_2} \frac{1}{N^{R_2}} \rightarrow 0 \quad (43)$$

with  $R_1, R_2 > 0$ .

### 5.5.3 Subsequent rounds

The same arguments apply in all subsequent rounds. That is, if in round  $m$  we allow a circuit depth of

$$L^{(m)}(N) = C_m \log(N), \quad (44)$$

with

$$C_m = \frac{-(1+R_m)}{\log \left( 1 - \frac{|G_{M-(m-1)}|}{|G_{M-m}|} \right)} \quad (45)$$

and  $R_m > 0$ , then, as the protocol terminates after  $M$  rounds, the probability that the protocol fails converges to zero as  $N \rightarrow \infty$ . Combined with the resource analysis from the Section 5.3, this demonstrates that it is possible to convert nilpotent SPT phases to the trivial phase asymptotically deterministically with symmetry preserving CMF.

## 6 Trivialization of non-normal phases

In this section, we show the trivialization of the non-normal (or GHZ) phases. To begin, the protocol used to transform the SPT state into the trivial phase also applies to the GHZ state. In this case, the probability distribution of measurement outcomes in each round remains uniform, subject to a parity constraint (see Appendix D). Therefore, the same protocol applies.

Performing the reverse transformation—preparing the GHZ state from a product state—requires additional considerations. In essence, the protocol proceeds as follows (see Fig. 3 for an example, cf. Ref. [29] for abelian symmetries): First, we locally prepare the fiducial state defined in Eq. (1) of the GHZ tensor. We then wish to perform a Bell-type measurement on adjacent virtual sites to obtain a GHZ state. However, since the state is locally supported on non-abelian subspaces of  $U_g^{\otimes 2}$ , we first employ an approach similar to the one used in the SPT protocol to successively reduce the support to abelian subspaces. In contrast to the SPT case, the outcomes do not admit a parity constraint. Therefore, we iteratively introduce auxiliary qubits, which are measured until the required parity constraint is satisfied. Crucially, we demonstrate that  $O(\log(N))$  auxiliary systems are

sufficient to ensure the probability of failure converges to zero. Finally, we perform a Bell-type measurement, including appropriate local corrections, to obtain the desired GHZ state. In the following, we analyze the resource requirements, examine the probability distribution of measurement outcomes, and show that, when restricted to a cumulative circuit depth of  $O(\log(N))$ , the probability of success approaches one in the thermodynamic limit.

## 6.1 Representative for the phase

In order to choose a representative of the GHZ phase, we again begin with the virtual symmetry. We require the action of the symmetry in the virtual space to be given by the linear regular-representation,

$$U_g^{\text{reg}} = \sum_{h \in G} |g \circ h\rangle \langle h|. \quad (46)$$

Thus, we take  $U_g^{\text{reg}}$  as the corresponding physical symmetry and select the  $N$ -partite  $|G|$ -dimensional GHZ state as the representative for the phase:

$$|\text{GHZ}_n\rangle = \sum_{g \in G} |gg\dots g\rangle. \quad (47)$$

Before presenting the protocol, we briefly summarize some useful properties of the abelian subspace of the regular representation. Let us define the operators

$$Z^\alpha = \sum_{h \in G} \chi_{h^{-1}}^\alpha |h\rangle \langle h|, \quad X_g = \sum_{h \in G} |h \circ g\rangle \langle h|, \quad (48)$$

where  $\alpha \in \text{Irr}_1$  labels the 1D irreps of  $G$  and  $g \in G$ . These operators act analogously to generalized Pauli matrices, satisfying  $[U_g, X_h] = 0$  and  $U_g Z^\alpha = \chi_g^\alpha Z^\alpha U_g$  for all  $g, h \in G$ ,  $\alpha \in \text{Irr}_1$ . We then have the following observation (see Ref. [29] for a proof).

**Observation 2.** *The vectors*

$$|\phi_{\alpha g_2 \dots g_n}\rangle = (Z^\alpha \otimes X_{g_2} \otimes \dots \otimes X_{g_n}) |\text{GHZ}_n\rangle, \quad (49)$$

with  $\alpha \in \text{Irr}_1$ , and  $g_2, \dots, g_n \in G$ , form a symmetric orthonormal basis for the abelian subspace of  $(U_g^{\text{reg}})^{\otimes n}$  and

$$(U_g^{\text{reg}})^{\otimes n} |\phi_{\alpha g_2 \dots g_n}\rangle = \chi_g^\alpha |\phi_{\alpha g_2 \dots g_n}\rangle. \quad (50)$$

## 6.2 Protocol

We now present in detail the three parts of the protocol preparing the GHZ state from a product state. An example of the protocol for the class-4 nilpotent group  $D_{32}$  is shown in Figs. 3 and 4. The protocol proceeds in three parts.

### 6.2.1 Part 1

We begin by locally preparing, on each site, the fiducial state defined in Eq. (1) of the GHZ tensor. We

will refer to the left and right leg of the fiducial states as the auxiliary qudits and the central leg as the physical qudit. Then we use a depth-2 circuit to move each right auxiliary qudit to its right neighbor. Throughout this protocol, we will only measure the auxiliary qudits, never the physical qudits—those will later hold the target state. The goal of Part 1 of the protocol is to reduce the support on auxiliary qudits to the abelian subspace on which we can then perform a Bell-type measurement.

To achieve this, we proceed as follows: In each round  $m \in \{1, \dots, M-1\}$ , we project onto the subspaces corresponding to the irreps within the equivalence classes of  $\text{Irr}_{M-(m-1)}/\sim$ , following the approach used in the SPT case. Since the measurements act only on subsets of the qudits—rather than on a pure state—we do not encounter the same parity constraints observed in the SPT scenario (for further details, see Section 6.4). However, we can still decompose each measurement outcome  $\mathbf{z}^{(m)}$  into minimal connected substrings that multiply to the identity, except possibly for the final substring, which need not multiply to the identity (as illustrated in Fig. 3(b)). Moreover, the substrings that do multiply to the identity can be again rearranged using a SWAP circuit, and further decomposed into substrings of length at most  $|G_{M-m}|/|G_{M-(m-1)}|$ . Similar to the SPT case, the protocol fails in round  $m$  if the required circuit depth exceeds  $L^{(m)}(N^{(m)})$ . Prior to performing the Bell-type measurement, we must ensure an overall parity constraint, which is the goal of Part 2.

### 6.2.2 Part 2

If the protocol succeeds in Part 1, we have obtained a state in which almost all auxiliary qubits have been grouped into supersites of size  $O(1)$  that have support solely on abelian subspaces, except for possibly  $O(1)$  auxiliary sites at the end of the chain. These sites can have support on any equivalence class of irreps at any level of the hierarchy. For example, if the measurement outcomes in the first round did not multiply to the identity, then the last  $O(|G_{M-1}|/|G_M|)$  pairs of auxiliaries will have support on irreps in non-identity equivalence classes in  $\text{Irr}_M/\sim$ . In general, we can define a “remainder” as the extent to which the measurement outcomes in each round fail to satisfy the parity constraint. This remainder can be represented by a tuple,  $\mathbf{y} = (y_2, \dots, y_M)$ , where each  $y_k$  is either a string of elements of  $\text{Irr}_k/\sim$  such that no subset multiplies to the identity, or  $y_k$  is the empty set,  $\emptyset$ , indicating that in round  $M-(k-1)$  the measurements failed to satisfy the parity constraint. The goal of Part 2 is to transform the output of Part 1 to a state in which *all* sites are grouped into  $O(1)$  supersites with support on abelian subspaces, i.e., to a state with remainder  $\mathbf{y} = (\emptyset, \emptyset, \dots, \emptyset)$ .

To this end, we append pairs of auxiliary sites to the end of the chain and perform symmetric projective

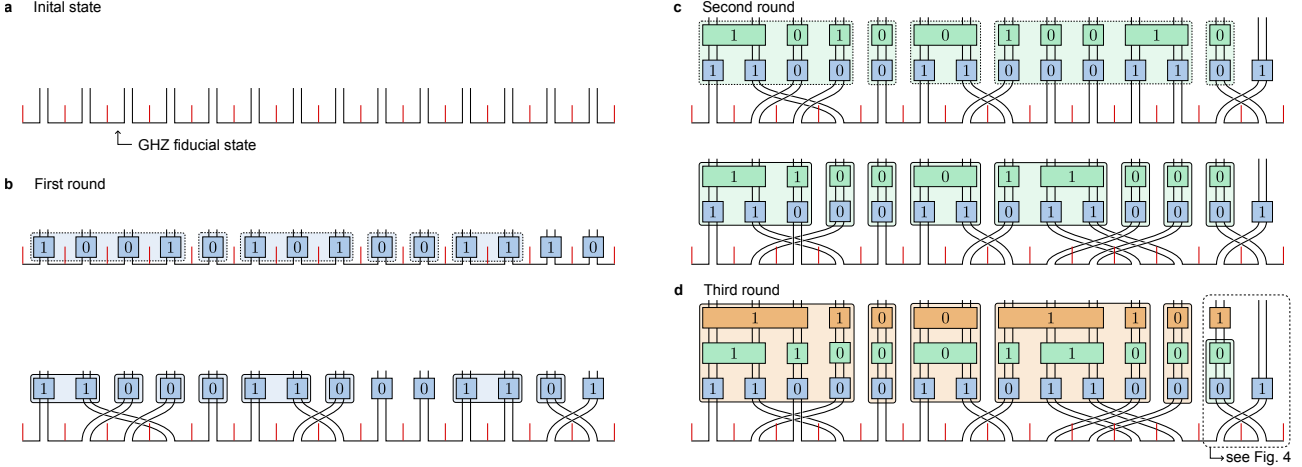


Figure 3: Example of Part 1 of the protocol transforming a state in the trivial phase to the GHZ state for the class-4 nilpotent group  $D_{32}$ —the dihedral group with thirty-two elements. For this group we have that the first three levels of the hierarchy are equipped with the group structure  $\text{Irr}_m \cong G_{m-1}/G_m \cong \mathbb{Z}_2$  for  $m = 4, 3, 2$ , i.e., the outcomes in each round can be labeled by  $0, 1 \in \mathbb{Z}_2$ . The protocol begins with the state in (a)—local copies of the fiducial state of the GHZ tensor, where the middle qudits, indicated by red lines, represent physical sites that remain untouched until the end of the protocol. Clearly the state is separable between sites and therefore in the trivial phase. After using a nearest-neighbor SWAP circuit to move each right auxiliary qudit to its right neighbor, the first round begins by performing measurements similar as in the SPT case. Note that, unlike the SPT case, the measurement outcomes are not guaranteed to multiply to the identity. Therefore, in each round, we have the possibility of a “remainder” parity. For example, in (b), the product of all measurement outcomes yields 1 instead of 0. As a result, there is a remainder at the end. The sites are permuted so that the remainder is moved to the end of the string. The protocol then proceeds to the next round, (c), leaving the remainder unmeasured until Part 2 of the protocol. Although measurement outcomes are not guaranteed to multiply to the identity, they may do so, as in (c), in which case there is no remainder. This is represented by  $\emptyset$  in the string  $y$  which denotes the remainder parity. For the above sequence of outputs,  $y = ((1), \emptyset, (1))$ . This concludes Part 1 of the protocol, for Part 2 see Fig. 4.

measurements to entangle the extra auxiliaries with the chain. These measurement operators can project the new auxiliary pair onto subspaces associated with any level of the hierarchy. As in Part 1 of the protocol, we can rearrange the sites at the end of chain and group them into supersites of size  $O(1)$  that multiply to the identity at some level of the hierarchy. We can then measure these supersites again in order to reach lower levels of the hierarchy as in Part 1. One can iteratively append sites, perform measurements, and rearrange sites until  $y = (\emptyset, \emptyset, \dots, \emptyset)$ . We now present an explicit protocol that accomplishes this in  $\log(N)$  rounds of measurements, each acting only on  $O(1)$  sites, interleaved with constant-depth circuits, resulting in an overall depth of  $O(\log(N))$ .

Before presenting the protocol, let us define the following measurement

$$\{P^{(n),k}\} = \{P_{[\alpha]}^{(n)}\}_{[\alpha] \in \text{Irr}_2/\sim} \cup \bigcup_{m=3,\dots,k} \{P_{[\alpha]}^{(n)}\}_{[\alpha] \in (\text{Irr}_m/\sim) \setminus [1]_m}. \quad (51)$$

This measurement extends the usual  $m = 2$  measurement,  $\{P_{[\alpha]}^{(n)}\}_{[\alpha] \in \text{Irr}_2/\sim}$ , with projectors onto the non-identity equivalence classes of irreps at each level  $m = k$ . We can label the outcome of this measurement by  $z = (z_2, z_3, \dots, z_M)$ , where  $z$  has only one entry that is not the empty set and which is an element of  $\text{Irr}_m/\sim$  for some  $m$ .

Equipped with this measurement, let us now describe the protocol in Part 2, see Fig. 4 for an example. Consider the case where  $y = (y_2, y_3, \dots, y_M) \neq (\emptyset, \emptyset, \dots, \emptyset)$ . First, we append the state  $|000\rangle$ , defined in Eq. (49), to the auxiliary site  $N$ . Now we perform the projective measurement  $\{P^{(2),M}\}$  on the right-most physical site and the auxiliary system with outcome  $z = (z_2, z_3, \dots, z_M)$ . In the example in Fig. 4(a) this corresponds to  $z = (\emptyset, 1, \emptyset)$  (green box). Let  $z_k$  be the entry of  $z$  that is not the empty set and consider the  $k^{\text{th}}$  entry of the remainder  $y$ , i.e.,  $y_k = (y_{ki})_i$ . If  $z_k \circ \prod_i y_{ki} = [1] \in \text{Irr}_k/\sim$ , we can rearrange the free sites and measure again, this time with  $\{P^{(2(l(y_k)+1)),k-1}\}$ , see Fig. 4(b). This corresponds to updating the remainder as  $y_k \mapsto \emptyset$  and produce a new output,  $z'$ , that has exactly one entry not equal to  $\emptyset$ , which is at entry strictly less than  $k$ . Similarly, if only a subset of  $S \subseteq y_k z_k$  multiplies to the identity, apply the above procedure to that subset only and update  $y \mapsto y_k z_k \setminus S$  accordingly. One can repeat this procedure until either no subset of  $y_k z_k$  multiplies to the identity or  $y_2 = \emptyset$ . If  $y = (\emptyset, \emptyset, \dots, \emptyset)$ , Part 2 terminates; otherwise, we repeat.

In this way, at the end of Part 2, the auxiliary qubits of the initial fiducial states can be partitioned into connected substrings of size  $O(|G|)$  that only have support on  $[1] \in \text{Irr}_2/\sim$ , i.e., the abelian subspace. Finally, we move the remaining physical site at the end

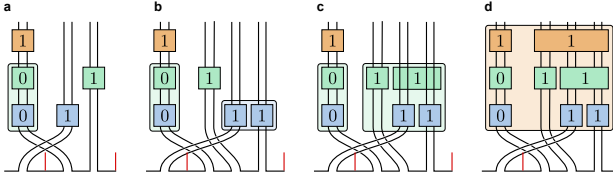


Figure 4: Example of Part 2 of the protocol, which establishes the parity constraint. At the end of Part 1 we can describe the remainder by  $\mathbf{y} = ((1), \emptyset, (1))$ ; see Fig. 3(d). (a) We append auxiliary systems in the state  $|\phi_{00}\rangle$  and perform the measurement  $P_{[\alpha]}^{(2),M}$ . The measurement outcome can belong to levels 2, 3 or 4 of the hierarchy. Let us assume we obtained an outcome belonging to  $\text{Irr}_2/\sim$  (green box). The remainder updates to  $\mathbf{y} = ((1), (1), (1))$ , where none of the  $y_i$  contain a subset whose elements multiply to the identity. Therefore, in (b), we rearrange the sites and append another auxiliary system in the state  $|\phi_{00}\rangle$ . We measure again, obtaining the updated remainder  $\mathbf{y} = ((1), (1), (1, 1))$ . Now  $y_2$  multiplies to the identity, so in (c) we perform another measurement, yielding  $\mathbf{y} = ((1), (1, 1), \emptyset)$ . Next,  $y_2$  multiplies to the identity, and in (d) we measure once more, obtaining  $\mathbf{y} = ((1, 1), \emptyset, \emptyset)$ . At this point, the total parity of the state is the identity, and we can proceed to Part 3.

of the chain back to site  $N$ .

### 6.2.3 Part 3

Now equipped with a state that can be decomposed into sites of size  $O(|G|)$  that only have support on the abelian subspace, we project onto the orthonormal basis for said subspace given in Observation 2. It can be verified, using similar arguments as in Sec. 5.4, that any state obtained after the measurement is equivalent to the desired GHZ state up to quasi-commuting local unitaries (see Appendix D). These can be corrected using local auxiliary systems [29].

## 6.3 Resources

Having verified that the protocol produces the desired state, let us review the resources required for the protocol.

First, let us consider the number of auxiliary systems we need per site and the maximum number of sites we must simultaneously measure. The protocol begins with at most three qudits per site. Part 1 requires no additional auxiliaries. Part 2, requires  $L^M$  auxiliaries. However, these are shared between  $L^M$  sites. We will ultimately choose  $L^M = O(\log(N)) < O(N)$ . Therefore, the protocol requires  $O(1)$  auxiliaries per site. Additionally, every measurement implemented during the protocol acts on  $O(1)$  sites.

As with the SPT case, each round in Part 1 requires  $O(|G_m|L^m)$  depth. In Part 2, we implement  $L^M$  rounds of measurements. In each round of measurements, the number of auxiliaries that require further measurements is at most  $|G_1|/|G_2| + \dots + |G_{M-1}|/|G_M|$ . Therefore, between each mea-

surement, we use  $O(1)$  depth circuits. Therefore, the cumulative depth of these actions is  $O(L^M)$ . Finally, at the end of Part 2, we move the physical qubit back to site  $N$ , thereby adding another depth- $O(L^M)$  circuit. Thus, the cumulative depth of Part 2 is  $O(L^M)$ , and therefore the cumulative depth of the protocol is  $\max_m O(\log^{(m)}(N))$ .

## 6.4 Probability distribution of measurement outcomes

The probability distribution for the measurements during the GHZ protocol is simpler than the SPT case. When evaluating the probability, analogous to Eq. (31), the unmeasured sites ensure that all  $b_{ijk}a_{ijk}$  terms conspire to equal identity. Consequently, one finds that the probability distribution is uniform, without any parity constraints. In particular, we have

$$p(\mathbf{x}^{(m)} | \mathbf{x}^{(1)}, \dots, \mathbf{x}^{(m-1)}) = \left( \frac{|G_{M-m-1}|}{|G_{M-m}|} \right)^{N^{(m)}}. \quad (52)$$

This also holds in Part 2 of the protocol as  $P_{[\alpha]_{m-1}}^{(n)} = P_{[\alpha]_{m-1}}^{(n)} P_{[1]_m}^{(n)}$ . For details, see Appendix E.

## 6.5 Probability of success

As in the SPT case, we restrict ourselves to circuits of depth  $O(\log(N))$  and show that the probability of success converges to 1 as  $N \rightarrow \infty$ . As the measurement outcome in each round of Part 1 are independent and identically distributed, the first part of the argument is identical to the SPT case—the protocol fails in round  $m$  if the measurement outcome contains a substring that is longer than  $L^{(m)}$ . As long as  $L^{(m)}$  is chosen to scale as  $O(\log(N))$ , with a sufficiently large constant prefactor, then the probability that the protocol fails during Part 1 vanishes as  $N \rightarrow \infty$ . In Part 2, the sequence of measurements can be viewed as a path on a finite Markov network, where each node corresponds to the possible value of  $\mathbf{y}$ . As the set of possible  $\mathbf{y}$  is finite and all trajectories eventually terminate at  $\emptyset$ , choosing  $L^{(M)}$  to grow with  $N$  ensures that the failure probability converges to zero. In particular,  $O(\log(N))$  is sufficient. Thus, combined with the resource analysis above, we have shown that it is possible to transform the trivial phase into the GHZ phase with asymptotically deterministic CMF for nilpotent groups.

## 7 Conclusion and Discussion

In this work, we have studied transformations of MPS under combinations of short-depth symmetric circuits and symmetric measurements, where the symmetry is with respect to a non-abelian nilpotent group. We explained that nilpotent groups have a powerful structure in their irreducible representations; namely, the

lower central series of a nilpotent group can be used to define a sequence of ascending subsets of irreducible representations,  $\text{Irr}_m$ , that can then be given a group structure,  $(\text{Irr}_m \sim, \circ)$ . This group structure is central in the construction of the protocols. This means that if one performs on-site measurements on subspaces associated with irreps contained in elements of  $\text{Irr}_m \sim$ , then one can combine the sites into supersites that only have support on subspaces associated with irreps in  $\text{Irr}_{m-1}$ . Using this, we showed that the trivial state can be asymptotically deterministically transformed into any SPT or GHZ-like state via circuits and measurements while respecting non-abelian nilpotent symmetries. Thus SPT and GHZ phases of non-abelian nilpotent groups trivialize with the inclusion of symmetric measurements.

Looking forward, it would be interesting to investigate whether phases of non-nilpotent non-abelian groups trivialize with the inclusion of symmetric measurements. This is not even clear for solvable groups - a simple class of non-abelian groups containing nilpotent groups. A direct application of our protocols to solvable groups does not work. For example, consider the non-nilpotent but solvable group  $S_3$ , the symmetric group on three elements. It has three irreps,  $\{1, 2, 3\}$ , of which only 3 is non-commutative. However,  $3 \otimes 3 \cong 1 \oplus 2 \oplus 3$ . That is, tensor products with a non-commutative irrep of  $S_3$  will always yield at least one non-commutative irrep. Therefore, combining non-commutative outcomes cannot yield a supersite with only support on abelian subspaces. It would also be interesting to go beyond finite groups.

## 8 Acknowledgments

We thank Maria Sharshunova for assistance with preparing the figures. DG, TK, and BK acknowledge financial support from the Austrian Science Fund (FWF) through the grants SFB BeyondC (Grant No. F7107-N38), and P 32273-N27 (Stand-Alone Project). Furthermore, we acknowledge the BMW endowment fund. This publication has received funding from the European Union's Horizon 2020 HORIZON Research and Innovation Actions Programme under the calls HORIZON-CL4-2022-QUANTUM-02-SGA via Grant Agreement No. 101113690 (PASQuanS2.1) and HORIZON-CL4-2021-DIGITAL-EMERGING-02-10 via Grant Agreement No. 101080085 (QCFD). GS acknowledges financial support by the Deutsche Forschungsgemeinschaft (DFG, German Research Foundation) under Germany's Excellence Strategy – EXC-2111 – 390814868.

## References

- [1] J. I. Cirac, D. Pérez-García, N. Schuch, and F. Verstraete, *Rev. Mod. Phys.* **93**, 045003 (2021).
- [2] X. Chen, Z.-C. Gu, and X.-G. Wen, *Phys. Rev. B* **83**, 035107 (2011).
- [3] N. Schuch, D. Pérez-García, and I. Cirac, *Phys. Rev. B* **84**, 165139 (2011).
- [4] X. Chen, Z.-C. Gu, and X.-G. Wen, *Phys. Rev. B* **82**, 155138 (2010).
- [5] M. B. Hastings and X.-G. Wen, *Phys. Rev. B* **72**, 045141 (2005).
- [6] B. Nachtergaelie, R. Sims, and A. Young, *J. Math. Phys.* **60**, 061101 (2019).
- [7] A. Coser and D. Pérez-García, *Quantum* **3**, 174 (2019).
- [8] R. Raussendorf and H. J. Briegel, *Phys. Rev. Lett.* **86**, 5188 (2001).
- [9] R. Raussendorf, S. Bravyi, and J. Harrington, *Phys. Rev. A* **71**, 062313 (2005).
- [10] M. Aguado, G. Brennen, F. Verstraete, and J. I. Cirac, *Phys. Rev. Lett.* **101**, 260501 (2008).
- [11] C. Meignant, D. Markham, and F. Grosshans, *Phys. Rev. A* **100**, 052333 (2019).
- [12] A. B. Watts, R. Kothari, L. Schaeffer, and A. Tal, in *Proc. Annu. ACM Symp. Theory Comput.*, STOC '19 (ACM, 2019) p. 515–526.
- [13] L. Piroli, G. Styliaris, and J. I. Cirac, *Phys. Rev. Lett.* **127**, 220503 (2021).
- [14] E. Chitambar, D. Leung, L. Mančinska, M. Ozols, and A. Winter, *Commun. Math. Phys.* **328**, 303 (2014).
- [15] D. T. Stephen and O. Hart, *Phys. Rev. B* **112**, 235127 (2025).
- [16] K. C. Smith, A. Khan, B. K. Clark, S. M. Girvin, and T.-C. Wei, *PRX Quantum* **5**, 030344 (2024).
- [17] R. Sahay and R. Verresen, *PRX Quantum* **6**, 010329 (2025).
- [18] D. Malz, G. Styliaris, Z.-Y. Wei, and J. I. Cirac, *Phys. Rev. Lett.* **132**, 040404 (2024).
- [19] N. Tantivasadakarn, R. Thorngren, A. Vishwanath, and R. Verresen, *Phys. Rev. X* **14**, 021040 (2024).
- [20] S. Bravyi, I. Kim, A. Kliesch, and R. Koenig, *arXiv:2205.01933* (2022).
- [21] T.-C. Lu, L. A. Lessa, I. H. Kim, and T. H. Hsieh, *PRX Quantum* **3**, 040337 (2022).
- [22] N. Tantivasadakarn, A. Vishwanath, and R. Verresen, *PRX Quantum* **4**, 020339 (2023).
- [23] Y. Li, H. Sukeno, A. P. Mana, H. P. Nautrup, and T.-C. Wei, *Phys. Rev. B* **108**, 115144 (2023).
- [24] Y. Zhang, S. Gopalakrishnan, and G. Styliaris, *PRX Quantum* **5**, 040304 (2024).
- [25] Y. Ren, N. Tantivasadakarn, and D. J. Williamson, *Phys. Rev. X* **15**, 031060 (2025).
- [26] M. Foss-Feig, A. Tikku, T.-C. Lu, K. Mayer, M. Iqbal, T. M. Gatterman, J. A. Gerber,

K. Gilmore, D. Gresh, A. Hankin, *et al.*, arXiv:2302.03029 (2023).

[27] M. Iqbal, N. Tantivasadakarn, R. Verresen, S. L. Campbell, J. M. Dreiling, C. Figgatt, J. P. Gaebler, J. Johansen, M. Mills, S. A. Moses, *et al.*, *Nature* **626**, 505 (2024).

[28] E. H. Chen, G.-Y. Zhu, R. Verresen, A. Seif, E. Bäumer, D. Layden, N. Tantivasadakarn, G. Zhu, S. Sheldon, A. Vishwanath, *et al.*, *Nat. Phys.* **21**, 161 (2025).

[29] D. Gunn, G. Styliaris, T. Kraft, and B. Kraus, *Phys. Rev. B* **111** (2025).

[30] S. Gelaki and D. Nikshych, *Adv. Math.* **217**, 1053 (2008).

[31] J. I. Cirac, D. Pérez-García, N. Schuch, and F. Verstraete, *Ann. Phys.* **378**, 100 (2017).

[32] M. Fannes, B. Nachtergael, and R. F. Werner, *Commun. Math. Phys.* **144**, 443 (1992).

[33] D. Pérez-García, F. Verstraete, M. M. Wolf, and J. I. Cirac, *Quantum Info. Comput.* **7**, 401 (2007).

[34] F. Pollmann, A. M. Turner, E. Berg, and M. Oshikawa, *Phys. Rev. B* **81**, 064439 (2010).

[35] M. Sanz, M. M. Wolf, D. Pérez-García, and J. I. Cirac, *Phys. Rev. A* **79**, 042308 (2009).

[36] The second cohomology group of a given subgroup,  $H \leq G$ , is a group property of  $H$ .

[37] Combination here is achieved by introducing an auxiliary site and using a low-depth circuit consisting of SWAP gates to exchange the auxiliary system with one of the measured sites.

[38] I. M. Isaacs, *Character theory of finite groups*, AMS Chelsea Publishing (American Mathematical Society, Providence, RI, 2006).

[39] D. S. Dummit and R. M. Foote, *Abstract Algebra* (John Wiley & Sons, 2003).

[40] J.-P. Serre, *Linear Representations of Finite Groups* (Springer New York, 1977).

[41] G. Karpilovsky, *Group Representations*, Group Representations No. Bd. 3 (Elsevier Science, 1994).

[42] The reason for that is that if the outcomes would multiply to any other equivalence class, then the projector onto it would be orthogonal to the input state. Hence, the outcomes on the first  $N-1$  sites determine the outcome of the last measurement. Note that a simple example of such a parity constraint is given in [29].

[43] S. Bereg, A. E. Holroyd, L. Nachmanson, and S. Pupyrev, *SIAM J. Discrete Math.* **30**, 1950 (2016).

[44] As an example, consider the string  $(1, 0, \dots, 0, 1)$ . If sufficiently large, this outcome contains an  $L^{(1)}$  substring, but due to periodicity the first and last site are nearest neighbors, and thus can be paired using a single SWAP gate.

[45] M. F. Schilling, *Coll. Math. J.* **21**, 196 (1990).

[46] We use italics label to indicate conjugacy classes. Each conjugacy class is a set of elements. The number of the label indicates the order of the elements in the class and the letter labels the different conjugacy classes with the same order.

## A Group structure of irreps of nilpotent groups

In this appendix, we show that the groups defined in the main text,  $(\text{Irr}_m / \sim, \circ)$ , are indeed a groups and are isomorphic to  $G_{m-1}/G_m$ . In fact, the way we will do this by first introducing a third group,  $(\text{Irr}_m / \sim_*, *)$ , and showing  $G_{m-1}/G_m \cong (\text{Irr}_m / \sim_*, *)$ . We will then show  $(\text{Irr}_m / \sim_*, *) = (\text{Irr}_m / \sim, \circ)$ .

### A.1 Proof of the isomorphism $(\text{Irr}_m / \sim_*, *) \cong G_{m-1}/G_m$

In this section, we introduce the group  $(\text{Irr}_m / \sim_*, *)$  and show its isomorphic to  $G_{m-1}/G_m$ . To begin, we define the equivalence relation  $\sim_*$ . To this end, let  $\alpha \in \text{Irr}_m$  be an irrep, and  $U_g^\alpha$  a unitary representation thereof. By the definition of  $\text{Irr}_m$  (see Eq. (10)), we have  $U_g^\alpha = \mathbb{1}$  for all  $g \in G_m$ . Thus, by definition of  $G_m$  and  $G_{m-1}$ , for every  $c \in G_{m-1}$  we have that  $(U_c^\alpha)^{-1}(U_h^\alpha)^{-1}U_c^\alpha U_h^\alpha = \mathbb{1}$  for all  $h \in G$ . Therefore, by Schur's lemma, we have that

$$U_c^\alpha = e^{i\tilde{\varphi}_c^\alpha} \mathbb{1}_{d^\alpha} \quad (53)$$

for all  $c \in G_{m-1}$ , where  $e^{i\tilde{\varphi}_c^\alpha}$  is a 1D irrep of  $G_{m-1}$  with kernel containing  $G_m$ . The map  $e^{i\varphi^\alpha} : G_{m-1}/G_m \rightarrow U(1)$  is the defined by quotienting out  $G_m$ :

$$e^{i\varphi_{[g]}^\alpha} = e^{i\tilde{\varphi}_g^\alpha}, \quad (54)$$

where  $[\cdot]$  denotes the canonical quotient map,  $[\cdot] : G_{m-1} \rightarrow G_{m-1}/G_m$ . It is easy to verify  $e^{i\varphi^\alpha}$  is well defined and an 1D irrep of  $G_{m-1}/G_m$ . Thus, we can define a map from  $\text{Irr}_m$  to the irreps of  $G_{m-1}/G_m$  by

$$\tilde{\Phi} : \alpha \mapsto e^{i\varphi^\alpha}. \quad (55)$$

We now show  $\tilde{\Phi}$  is surjective. To this end, let  $e^{i\phi} \in \text{Irr}(G_{m-1}/G_m)$  and let  $e^{i\tilde{\phi}} \in \text{Irr}(G_{m-1})$  be defined by  $e^{i\tilde{\phi}} = e^{i\phi} \circ \Pi$ , where  $\Pi$  is the canonical projection map. Now consider the representation of  $G$  induced [38] by

$e^{i\tilde{\phi}} \in \text{Irr}(G_{m-1})$ . That is, let  $k_i \in G$  be representative for the coset  $i \in G/G_{m-1}$  and define  $\xi(g, i)$  and  $h(g, i)$  by

$$gk_i = k_{\xi(g, i)} h(g, i). \quad (56)$$

Note that not only is  $G_m$  normal in  $G_{m-1}$ , it is also normal in  $G$ , and thus  $G/G_{m-1}$  is well-defined. Then the induced representation  $\text{Ind}_H^G e^{i\tilde{\phi}}$  is given by

$$\text{Ind}_{G_{m-1}}^G e^{i\tilde{\phi}}(g) = \sum_{i \in G/[G_{m-1}]} e^{i\tilde{\phi}}(h(g, i)) |\xi(g, i)\rangle \langle i| \quad (57)$$

It is easily verified that  $\text{Ind}_{G_{m-1}}^G e^{i\tilde{\phi}}$  is indeed a representation of  $G$  and therefore can be decomposed into irreps of  $G$ . Note, we also have

$$\text{Ind}_{G_{m-1}}^G e^{i\tilde{\phi}}(h) = e^{i\tilde{\phi}}(h) \mathbf{1}_{|G/G_{m-1}|} \quad (58)$$

for all  $h \in G_{m-1}$ . In particular therefore, all irreps in  $\text{Ind}_{G_{m-1}}^G e^{i\tilde{\phi}}$  are mapped to  $e^{i\phi}$  by  $\Phi$ . Therefore, there is an  $\alpha \in \text{Irr}_m$  such that  $\Phi(\alpha) = e^{i\phi}$ .

As  $\tilde{\Phi}$  is surjective, we can promote it to a bijective map by defining an equivalence relation  $\sim_*$  on  $\text{Irr}_m$ . Namely, we say that  $\alpha \sim_* \beta$  if  $\tilde{\Phi}(\alpha) = \tilde{\Phi}(\beta)$ . Clearly, this is an equivalence relation. We denote the equivalence class that  $\alpha \in \text{Irr}_m$  belongs to by  $[\alpha]$ . Then the map  $\Phi : \text{Irr}_m / \sim_* \rightarrow \text{Irr}(G_{m-1}/G_m)$  defined by

$$\Phi([\alpha]) = \tilde{\Phi}(\alpha) \quad (59)$$

is clearly a bijection, with  $\Phi^{-1}(1) = \text{Irr}_{m-1}$ .

Finally, we can equip the set of equivalence classes  $\text{Irr}_m / \sim_*$  with a group multiplication

$$[\alpha] * [\beta] \equiv \Phi^{-1}(\Phi([\alpha])\Phi([\beta])),. \quad (60)$$

where  $\Phi^{-1}$  is the pre-image. This clearly ensures  $\Phi$  is a group homomorphism and therefore, as its bijective, an isomorphism. We have thus proven that

$$(\text{Irr}_m / \sim_*, *) \cong \text{Irr} \left( \frac{G_{m-1}}{G_m} \right) \cong \frac{G_{m-1}}{G_m}, \quad (61)$$

where the last isomorphism follows from the fact that  $G_{m-1}/G_m$  is abelian and the fact finite abelian groups are isomorphic to their irreducible representations.

## A.2 Proof of the isomorphism $(\text{Irr}_m / \sim_*, *) = (\text{Irr}_m / \sim, \circ)$

We now show that the group  $(\text{Irr}_m / \sim, \circ)$  from the main text is in fact exactly the same as  $(\text{Irr}_m / \sim_*, *)$ . To begin, for convenience, let us recall the definition of  $(\text{Irr}_m / \sim, \circ)$ . As we will be later be comparing equivalence relations, let us use  $\sim_\circ$  to refer to the original equivalence relation, Eq. (11). That is, for  $\alpha, \beta \in \text{Irr}_m$ , we have

$$\beta \sim_\circ \alpha \text{ if } \exists \gamma \in \text{Irr}_{m-1} : \alpha \in \gamma \otimes \beta, \quad (62)$$

where  $\alpha \in \gamma \otimes \beta$  means that the irrep  $\alpha$  appears in the decomposition of  $\gamma \otimes \beta$ . Group multiplication is given by

$$[\alpha]_\circ \circ [\beta]_\circ = \{ \delta \in \text{Irr}_m : \exists \alpha' \in [\alpha]_\circ, \beta' \in [\beta]_\circ : \delta \in \alpha' \otimes \beta' \} \quad (63)$$

We will now show

$$(\text{Irr}_m / \sim_\circ, \circ) = (\text{Irr}_m / \sim_*, *) \quad (64)$$

Before showing this let us note the following observation

**Observation 3.** For all  $\alpha \in \text{Irr}$ , there is a unique irrep  $\alpha^{-1}$  such that  $1 \in \alpha \otimes \alpha^{-1}$ , namely the conjugate representation  $\alpha^{-1} = \alpha^*$ . Moreover,  $\text{Irr}_m = \text{Irr}_m^*$ .

*Proof.* The first statement is a consequence of Schur's lemma. To see this explicitly, let  $\alpha, \beta \in \text{Irr}$  then  $\alpha \otimes \beta \ni 1$  iff there is a non-zero vector  $|\psi\rangle = \psi \otimes \mathbf{1} |\phi^+\rangle$  such that  $U_g^\alpha \otimes U_g^\beta |\psi\rangle = |\psi\rangle$  for all  $g \in G$ . This holds iff  $U_g^\alpha \psi (U_g^\beta)^T = \psi$  which is equivalent to  $U_g^\alpha \psi = \psi (U_g^\beta)^*$ , for all  $g \in G$ . Thus by Schur's Lemma,  $\beta = \alpha^*$ . The statement that  $\text{Irr}_m = \text{Irr}_m^*$  follows trivially from the definition of  $\text{Irr}_m$ .  $\square$

Now let us show  $(\text{Irr}_m / \sim_0, \circ) = (\text{Irr}_m / \sim_*, *)$ .

*Proof.* First, let us verify that the equivalence classes are the same, i.e.,

$$\alpha \stackrel{\circ}{\sim} \beta \Leftrightarrow \alpha \stackrel{*}{\sim} \beta. \quad (65)$$

$(\Leftarrow)$ . If  $\alpha \stackrel{*}{\sim} \beta$ , then there is a  $\gamma \in \text{Irr}_{m-1}$  such that  $\alpha \in \gamma \otimes \beta$ . Now consider a unitary representation of  $\alpha, \beta$  and  $\gamma$  and consider the restriction to  $G_{m-1}$ . Recall we have

$$U_c^\alpha = e^{i\tilde{\phi}_c^\alpha} \mathbf{1}_{d^\alpha} \quad (66)$$

for all  $c \in G_{m-1}$  and likewise for  $\beta$  and  $\gamma$ . However,  $\gamma \in \text{Irr}_{m-1}$  and therefore  $e^{i\phi_c^\gamma} = 1$  and thus

$$U_c^\gamma \otimes U_c^\beta = e^{i\tilde{\phi}_c^\beta} \mathbf{1}_{d^\gamma d^\beta} \quad (67)$$

for all  $c \in G_{m-1}$ . As  $\alpha \in \gamma \otimes \beta$ , this means  $e^{i\tilde{\phi}_c^\beta} = e^{i\tilde{\phi}_c^\alpha}$  and thus

$$\exp(i\phi_{[c]}^\alpha) = \exp(i\phi_{[c]}^\beta), \quad (68)$$

for all  $[c] \in G_{m-1}/G_m$ . Thus  $\alpha \stackrel{\circ}{\sim} \beta$ .

$(\Rightarrow)$ . Now let  $\alpha \stackrel{\circ}{\sim} \beta$ , i.e.,  $\exp(i\phi_{[g]}^\beta) = \exp(i\phi_{[g]}^\alpha)$ . Considering  $c \in G_{m-1}$ , it is clear if we tensor the conjugate of  $\alpha$  with  $\beta$  we have that  $(U_c^\alpha)^* \otimes U_c^\beta = \mathbf{1}_{d^\alpha d^\beta}$ . Thus, by the definition of  $\text{Irr}_{m-1}$ , all irreps in the decomposition belong to  $\text{Irr}_{m-1}$ ,  $\alpha^* \otimes \beta \subseteq \text{Irr}_{m-1}$ . Let  $\gamma \in \text{Irr}_{m-1}$  be one such irrep, i.e.,  $\gamma \in \alpha^* \otimes \beta$ . Then we must have  $1 \in \alpha^* \otimes (\gamma^* \otimes \beta)$ . As  $\gamma^* \otimes \beta$  decomposes into irreps, i.e.,  $\gamma^* \otimes \beta = \bigoplus_i \delta_i$ , and then  $\alpha^* \otimes (\gamma^* \otimes \beta) \cong \bigoplus_i (\alpha^* \otimes \delta_i) \ni 1$ , this means, by Obs. 3, at least one of the irreps  $\delta_i$  must be  $\alpha$ . Therefore,  $\alpha \in \gamma^* \otimes \beta$ , with  $\gamma^* \in \text{Irr}_{m-1}$ , and thus,  $\alpha \stackrel{*}{\sim} \beta$ .

Having verified that the equivalences classes are the same, let us now verify the group multiplication is the same, i.e.,

$$[\alpha] \circ [\beta] = [\alpha] * [\beta] \quad (69)$$

Note, both the left and right hand sides are sets. Thus, we show they are equivalent by showing they are subsets of one another.

$(\supseteq)$ . Let  $\delta \in [\alpha] * [\beta]$ . Then  $\exists \alpha' \in [\alpha], \beta' \in [\beta]$  such that  $\delta \in \alpha' \otimes \beta'$ . Again considering restrictions to  $G_{m-1}$ , it is therefore clear that

$$\exp(i\phi_{[g]}^\gamma) = \exp(i\phi_{[g]}^\alpha) \exp(i\phi_{[g]}^\beta) \quad (70)$$

and, thus,  $\gamma \in [\alpha] \circ [\beta]$ .

$(\subseteq)$ . Let  $\gamma \in [\alpha] \circ [\beta]$ . That is  $\exp(i\phi_{[g]}^\gamma) = \exp(i\phi_{[g]}^\alpha) \exp(i\phi_{[g]}^\beta)$ . Therefore, we have  $\gamma^* \otimes (\alpha \otimes \beta) \subseteq \text{Irr}_{m-1}$ . Let  $\delta \in \gamma^* \otimes (\alpha \otimes \beta)$ . Thus,  $1 \in \gamma^* \otimes ((\delta^* \otimes \alpha) \otimes \beta)$ . Note, by definition  $\delta^* \otimes \alpha \in [\alpha]$ . Therefore, defining  $\alpha' = \delta^* \otimes \alpha$ , by Obs 3, we have  $\gamma \in \alpha' \otimes \beta$ . Thus  $\gamma \in [\alpha] * [\beta]$ .  $\square$

Thus,  $(\text{Irr}_m / \sim, \circ)$  is a group isomorphic to  $G_{m-1}/G_m$ . Considering the definitions in Eq. (62) and Eq. (63), it is clear that  $[1]_m = \text{Irr}_{m-1}$  is the group identity element. Moreover, by Observation 3 we have that  $[\alpha]^{-1} = [\alpha]^*$ .

## B Example of the group structure of irreps of nilpotent groups

In this appendix, we illustrate the structure of the groups  $(\text{Irr}_m / \sim, \circ)$ . As an example, we consider  $G = D_{16}$ , the dihedral group of order 16. By examining the successive commutator groups,  $G_{m+1} = [G_m, G]$ , we obtain the lower central series

$$D_{16} \triangleright \mathbb{Z}_4 \triangleright \mathbb{Z}_2 \triangleright 1, \quad (71)$$

and therefore,  $G$  is a class-3 nilpotent group. The abelian factor groups,  $G_{m-1}/G_m$ , representing the group structures of  $(\text{Irr}_m / \sim, \circ)$ , are therefore given by  $K_4, \mathbb{Z}_2$ , and  $\mathbb{Z}_2$ .

## B.1 The hierarchy of irreps

Let us begin by constructing the sets,  $\text{Irr}_m$ , of irreps in Eq. (9) in the main text. Recall, that  $\text{Irr}_m$  consists of those irreps that act trivially for all  $g \in G_m$ , see Eq. (10). Equivalently, it contains those irreps whose kernels contain  $G_m$ , with the kernel of an irrep being defined by  $\ker(\alpha) = \{g \in G : U_g^\alpha = \mathbf{1}\}$ . Those kernels, and subsequently the sets  $\text{Irr}_m$ , can be identified from the below character table of  $D_{16}$ . Here, the rows, labeled by  $\alpha$ , correspond to the different irreps and the columns correspond to the conjugacy classes of  $G$  [46].

$\alpha$	1	$2a$	$2b$	$2c$	4	$8a$	$8b$
1	1	1	1	1	1	1	1
2	1	1	-1	1	1	-1	-1
3	1	1	1	-1	1	-1	-1
4	1	1	-1	-1	1	1	1
5	2	2	0	0	-2	0	0
6	2	-2	0	0	0	$\sqrt{2}$	$-\sqrt{2}$
7	2	-2	0	0	0	$-\sqrt{2}$	$\sqrt{2}$

The kernel of an irrep  $\alpha$  is given by those elements for which  $\chi(g) = \chi(1)$ . Then, to check if a kernel contains  $G_m$ , we express  $G_m$  in terms of conjugacy classes

$$Z_4 \cong 1 \cup 2a \cup 4 \quad (73)$$

$$Z_2 \cong 1 \cup 2a \quad (74)$$

$$1 \cong 1. \quad (75)$$

By inspecting the character table it is then easily verified that the corresponding hierarchy of irreps is given by

$$\text{Irr}_0 = \{1\} \quad (76)$$

$$\text{Irr}_1 = \{1, 2, 3, 4\} \quad (77)$$

$$\text{Irr}_2 = \{1, 2, 3, 4, 5\} \quad (78)$$

$$\text{Irr}_3 = \{1, 2, 3, 4, 5, 6, 7\} = \text{Irr}. \quad (79)$$

## B.2 Group structure

Next, to identify corresponding equivalence classes we need to consider tensor products of irreps and their decompositions. We find the following:

$\otimes$	1	2	3	4	5	6	7
1	1	2	3	4	5	6	7
2	2	1	4	3	5	7	6
3	3	4	1	2	5	7	6
4	4	3	2	1	5	6	7
5	5	5	5	5	$1 \oplus 2 \oplus 3 \oplus 4$	$6 \oplus 7$	$6 \oplus 7$
6	6	7	7	6	$6 \oplus 7$	$1 \oplus 4 \oplus 5$	$2 \oplus 3 \oplus 5$
7	7	6	6	7	$6 \oplus 7$	$2 \oplus 3 \oplus 5$	$1 \oplus 4 \oplus 5$

To form equivalence classes in  $\text{Irr}_m$  under the equivalence relation stated in Eq. (11) in the main text, we consider the irreps in  $\text{Irr}_m$  and their tensor products by irreps in  $\text{Irr}_{m-1}$ . For instance, for  $m = 3$ ,  $\text{Irr}_m = \text{Irr}$ . Consider the irreps 5 and 1. Clearly, there is an irrep,  $\gamma$ , in  $\text{Irr}_{m-1} = \{1, 2, 3, 4, 5\}$  that such that  $\gamma \otimes 5 \ni 5$  (namely 1). Conversely,  $5 \in \text{Irr}_{m-1}$  and  $5 \otimes 5 \ni 1$ . Thus,  $1 \sim 5$ . Continuing this analysis, yields a partitioning of each  $\text{Irr}_m$  by the equivalence class described above, yielding

$$\text{Irr}_0 / \sim = \{\{1\}\} \quad (81)$$

$$\text{Irr}_1 / \sim = \{\{1\}, \{2\}, \{3\}, \{4\}\} \quad (82)$$

$$\text{Irr}_2 / \sim = \{\{1, 2, 3, 4\}, \{5\}\} \quad (83)$$

$$\text{Irr}_3 / \sim = \{\{1, 2, 3, 4, 5\}, \{6, 7\}\}. \quad (84)$$

Now, to see the group structure, consider as an example  $\text{Irr}_3/\sim$ . According to the above analysis, we should have  $\text{Irr}_3/\sim \cong \mathbb{Z}_2$ . To see this consider tensor products of irreps. We have

$$1 \otimes 6 = 4 \otimes 6 = 2 \otimes 7 = 3 \otimes 7 = 6 \in \{6, 7\} \quad (85)$$

$$1 \otimes 7 = 4 \otimes 7 = 2 \otimes 6 = 3 \otimes 6 = 7 \in \{6, 7\} \quad (86)$$

$$5 \otimes 5 = 6 \oplus 7 \subseteq \{6, 7\}. \quad (87)$$

Thus, we can see that  $\{1, 2, 3, 4, 5\} \circ \{6, 7\} = \{6, 7\}$ . It is similarly verified that  $\{1, 2, 3, 4, 5\} \circ \{1, 2, 3, 4, 5\} = \{1, 2, 3, 4, 5\}$  and  $\{6, 7\} \circ \{6, 7\} = \{1, 2, 3, 4, 5\}$ . Then,  $\text{Irr}_3/\sim$  is indeed isomorphic to  $\mathbb{Z}_2$ . Similarly, it is easy to verify that  $\text{Irr}_1/\sim \cong G_0/G_1 \cong K_4$  and  $\text{Irr}_2/\sim \cong G_1/G_2 \cong \mathbb{Z}_2$ . Moreover, we can verify that  $[1]_m = \text{Irr}_{m-1}$  acts as the identity element for each  $m$ .

### B.3 Projectors

Finally, let us continue with  $G = D_{16}$  and consider a example of Eq. (6), which we restate for convenience:

$$P_{[\alpha]_m}^{(n)} \otimes P_{[\beta]_m}^{(n')} \subseteq P_{[\alpha]_m \circ [\beta]_m}^{(n+n')}. \quad (88)$$

To simplify things, consider an onsite symmetry  $U_g = 1 \oplus 6 \oplus 7$  (the following also holds for any representation, including the regular representation, but demonstrating the notation for larger examples is tedious). Then

$$P_{[1]_M}^{(1)} = (1)_1 \oplus (0_2)_6 \oplus (0_2)_7 \quad (89)$$

$$P_{[2]_M}^{(1)} = (0)_1 \oplus (\mathbb{1}_2)_6 \oplus (\mathbb{1}_2)_7, \quad (90)$$

where the subscripts label the irreps associated with the subspace, and  $0_2$  is shorthand for a  $2 \times 2$  zero matrix. Then

$$P_{[2]_M}^{(1)} \otimes P_{[2]_M}^{(1)} = (0 \otimes 0)_{1 \otimes 1} \oplus (0 \otimes \mathbb{1}_2)_{1 \otimes 6} \oplus (0 \otimes \mathbb{1}_2)_{1 \otimes 7} \quad (91)$$

$$(\mathbb{1}_2 \otimes 0)_{6 \otimes 1} \oplus (\mathbb{1}_2 \otimes \mathbb{1}_2)_{6 \otimes 6} \oplus (\mathbb{1}_2 \otimes \mathbb{1}_2)_{1 \otimes 7} \quad (92)$$

$$(\mathbb{1}_2 \otimes 0)_{7 \otimes 1} \oplus (\mathbb{1}_2 \otimes \mathbb{1}_2)_{7 \otimes 6} \oplus (\mathbb{1}_2 \otimes \mathbb{1}_2)_{7 \otimes 7} \quad (93)$$

$$\subseteq (1)_{1 \otimes 1} \oplus (0_2)_{1 \otimes 6} \oplus (0_2)_{1 \otimes 7} \quad (94)$$

$$(0_2)_{6 \otimes 1} \oplus (1 \oplus 1 \oplus \mathbb{1}_2)_{6 \otimes 6} \oplus (1 \oplus 1 \oplus \mathbb{1}_2)_{1 \otimes 7} \quad (95)$$

$$(0_2)_{7 \otimes 1} \oplus (1 \oplus 1 \oplus \mathbb{1}_2)_{7 \otimes 6} \oplus (1 \oplus 1 \oplus \mathbb{1}_2)_{7 \otimes 7} \quad (96)$$

$$= P_{[1]_M}^{(2)}, \quad (97)$$

where in the third line we have decomposed  $6 \otimes 6 = 7 \otimes 7 = 1 \oplus 4 \oplus 5$  and  $6 \otimes 7 = 7 \otimes 6 = 2 \oplus 3 \oplus 5$ . Thus,  $P_{[2]_M}^{(1)} \otimes P_{[2]_M}^{(1)}$  only has support on subspaces associated with irreps in  $\text{Irr}_{M-1} = [1]_M = [2]_M \circ [2]_M$ . Note, that  $P_{[2]_M}^{(1)} \otimes P_{[2]_M}^{(1)} \neq P_{[1]_M}^{(2)}$ .

## C Proof of Lemma 1

In this section, we prove Lemma 1, which we restate here for convenience.

**Lemma 1.** *Let  $\text{Irr}_m/\sim \cong G_{m-1}/G_m = \{[\alpha]\}$ , and  $\Phi : \text{Irr}_m/\sim \rightarrow \text{Irr}(G_{m-1}/G_m)$  as defined in Eq. (59) with  $\Phi([\alpha]) = e^{i\varphi^{[\alpha]}}$ . Then,*

$$P_{[\alpha]}^{(n)} = \sum_{g \in G_{m-1}} \frac{e^{-i\varphi^{[\alpha]}([g])}}{|G_{m-1}|} U_g^{\otimes n}. \quad (98)$$

*Proof.* Let  $[\alpha] \in \text{Irr}_m/\sim \cong G_{m-1}/G_m$ . We have, by Eq. (15) in the main text, that

$$P_{[\alpha]}^{(n)} = \sum_{\alpha \in [\alpha]} P_{\alpha}^{(n)} = \sum_{\alpha \in [\alpha]} \sum_{g \in G} \frac{d^{\alpha} \bar{\chi}_g^{\alpha}}{|G|} U_g^{\otimes n}. \quad (99)$$

Let  $e^{i\tilde{\phi}^{\alpha}} \in \text{Irr}(G_{m-1})$  be defined by  $e^{i\phi^{[\alpha]}} \equiv e^{i\tilde{\phi}^{\alpha}} \circ \Pi$ , where  $\Pi$  is the canonical projection from  $G_{m-1}$  to  $G_{m-1}/G_m$ . We will prove the Lemma by proving the following:

$$\sum_{\alpha \in [\alpha]} \frac{d^{\alpha} \bar{\chi}_g^{\alpha}}{|G|} = \frac{e^{-i\varphi^{[\alpha]}([g])}}{|G_{m-1}|} \delta_{g \in G_{m-1}}. \quad (100)$$

The proof proceeds by relating both sides of the above equation to the character of the induced representation  $\text{Ind}_{G_{m-1}}^G e^{i\tilde{\phi}^\alpha}$  (cf. Eq. (57)). It is easy to verify that its character is given by

$$\text{tr} \left[ \text{Ind}_{G_{m-1}}^G e^{i\tilde{\phi}^\alpha} (g) \right] = e^{i\phi^{[\alpha]}} \frac{|G|}{|G_{m-1}|} \delta_{g \in G_{m-1}}. \quad (101)$$

Another way of expressing the character can be obtained as follows: Due to Eq. (58), all irreps in  $\text{Ind}_{G_{m-1}}^G e^{i\tilde{\phi}^\alpha}$  belong to  $[\alpha]$ . For any  $\alpha' \in [\alpha]$  we can compute its multiplicity,  $m^{[\alpha]}(\alpha')$ , in the induced representation  $\text{Ind}_{G_{a-1}}^G e^{i\tilde{\phi}^\alpha}$ . By simple character theory, we have that

$$m^{[\alpha]}(\alpha') = \frac{1}{|G|} \sum_{g \in G} \bar{\chi}_g^{\alpha'} \text{tr} \left[ \text{Ind}_{G_{m-1}}^G e^{i\tilde{\phi}^\alpha} (g) \right] \quad (102)$$

$$= \frac{1}{|G|} \sum_{g \in G} \bar{\chi}_g^{\alpha'} \left[ e^{i\phi^{[\alpha]}} \frac{|G|}{|G_{m-1}|} \delta_{g \in G_{m-1}} \right] \quad (103)$$

$$= \frac{1}{|G_{m-1}|} \sum_{g \in G_{m-1}} d^{\alpha'} e^{-i\phi_g^{[\alpha]}} [e^{i\phi_g^{[\alpha]}}] \quad (104)$$

$$= d^{\alpha'} \quad (105)$$

That is, every irrep  $\alpha' \in [\alpha]$  appears in  $\text{Ind}_{G_{m-1}}^G e^{i\tilde{\phi}^\alpha} (g)$  with multiplicity equal to its dimension. Therefore, we can write

$$\text{Ind}_{G_{m-1}}^G e^{i\tilde{\phi}^\alpha} (g) \cong \bigoplus_{\alpha' \in [\alpha]} (U_g^{\alpha'})^{\oplus d^{\alpha'}}, \quad (106)$$

where  $U_g^\alpha$  is some canonical unitary representation of the irrep  $\alpha$ . Thus, we can also express the character as

$$\text{tr} \left[ \text{Ind}_{G_{m-1}}^G e^{i\tilde{\phi}^\alpha} (g) \right] = \sum_{\alpha' \in [\alpha]} d^{\alpha'} \chi_g^{\alpha'} = e^{i\phi^{[\alpha]}} \frac{|G|}{|G_{m-1}|} \delta_{g \in G_{m-1}}. \quad (107)$$

Taking the conjugate of both sides of this last equality, we have Eq. (100) and hence the lemma.  $\square$

## D GHZ protocol: Verification of the final state

In this appendix, we show that the protocol in Section 6 outputs a state locally symmetric-unitary equivalent to the desired GHZ state. For simplicity, let us consider a class-3 nilpotent group. It will be clear how the construction extends to larger classes. Additionally, let us consider the case where no Part 2 is required and no circuits are needed; that is, in Part 1, the measurement outcomes conspire so that each measurement output,  $\mathbf{x}^{(m)}$ , already decomposes into substrings of length at most  $|G_{M-m}|/|G_{M-(m-1)}|$  that multiply to identity. We will address the effect of Part 2 and permutation circuits at the end of the section.

Due to this assumption, we may write the outcomes of the first two measurement rounds as

$$\mathbf{x}^{(2)} = (\mathbf{x}_i^{(2)})_{i=1}^{N^{(3)}} = ((x_{ij}^{(2)})_{j=1}^{N_i^{(2)}})_{i=1}^{N^{(3)}} \quad (108)$$

$$\mathbf{x}^{(1)} = (\mathbf{x}_i^{(1)})_{i=1}^{N^{(3)}} = ((x_{ij}^{(1)})_{j=1}^{N_i^{(2)}})_{i=1}^{N^{(3)}} = (((x_{ijk}^{(1)})_{k=1}^{N_{ij}^{(1)}})_{j=1}^{N_i^{(2)}})_{i=1}^{N^{(3)}} \quad (109)$$

where (see Fig. 5)

$$\circ_k x_{ijk}^{(1)} = [1] \in \text{Irr}_{M=3} / \sim, \quad \forall ij \quad (110)$$

$$\circ_j x_{ij}^{(2)} = [1] \in \text{Irr}_{(M-1)=2} / \sim, \quad \forall i. \quad (111)$$

Note, that we use the upper index to refer to the measurement round, and the lower multi-index to refer to the partitioning (and subpartitioning) of the string of measurement outcomes according to how they multiply to the identity. The lower index is a multi-index, so, for example,  $x_{11N_{11}^{(1)}}^{(1)}$  is followed by  $x_{121}^{(1)}$ , which is followed by  $x_{122}^{(1)}$ , and so on.

Then, in the last round of the protocol, on supersites corresponding to each  $\mathbf{x}_i^{(2)}$  for each  $i \in \{1, \dots, N^{(3)}\}$ , we project the 1D subspaces of  $U_g^{\otimes n'}$ , where  $n' = \sum_j 2N_{ij}$  (see Fig. 5). The eigenvectors of these 1D subspaces

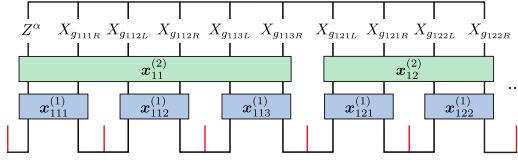


Figure 5: Example of projective measurements on the first substring of sites in round 3 for a class-3 Nilpotent group (assuming no permutation circuits are required). Let us discuss this image as an aid to understanding the notation introduced. Looking at this image, we can read off the measurement history of the protocol. Starting from the top of the image, we see the final projective measurement, corresponding to Eq. (113). Moving down, there were two projective measurements (green boxes) in round two. Thus, these two measurements must have totaled to identity; i.e.,  $N_1^{(2)} = 2$  and  $x_{11}^{(2)} \circ \dots \circ x_{1N_1^{(2)}}^{(2)} = [1]$ . Looking under the first round-two-measurement,  $x_{11}^{(2)}$ , we see three round one measurements (blue boxes). Thus, these measurements must have totaled to identity; i.e.,  $N_{11}^{(1)} = 3$  and  $x_{111}^{(1)} \circ \dots \circ x_{1N_{11}^{(1)}}^{(1)} = [1]$ . Note, this is just the first substring ( $i = 1$ ); the state continues to the right.

are given in Obs. 2, which we restate for ease of reading. First, we define  $Z^\alpha = \sum_{h \in G} \chi_{h^{-1}}^\alpha |h\rangle\langle h|$  and  $X_g = \sum_{h \in G} |h \circ g\rangle\langle h|$ . Recall,  $Z^\alpha$  and  $X_g$  are quasi-commuting with  $U_g$ . Then the common eigenvectors of  $U_g^{\otimes n}$  are given by

$$|\phi_{\alpha g_2 \dots g_n}\rangle = (Z^\alpha \otimes X_{g_2} \otimes \dots \otimes X_{g_n}) |\text{GHZ}_n\rangle. \quad (112)$$

Recall, throughout the protocol, we only measure on the auxiliary qudits of the fiducial state. Therefore  $g_{ijkL}$  corresponds to the left auxiliary qudit and  $g_{ijkR}$  corresponds to the right auxiliary qudit. Thus, using the notation introduced above, in the last round we project onto

$$|\alpha_i, g_{i11R}, g_{i12L}, g_{i12R}, \dots, g_{iN_i^{(2)} N_{iN_i^{(1)}}^{(1)} L}, g_{iN_i^{(2)} N_{iN_i^{(1)}}^{(1)} R}\rangle \quad (113)$$

for each  $i \in \{1, \dots, N^{(3)}\}$  (see Fig. 5).

We will now show that the state after this projection is, up to on-site quasi-commuting local unitaries, the GHZ state. As we consider the case where no circuits are needed, we may consider the qudits associated with each substring  $x_i^{(2)}$  in turn. Let us evaluate the first ( $i = 1$ ) substring, an example of which is depicted in Fig. 5. To this end, we use decomposition of the projectors  $P_{[\alpha]}^{(n)}$  at level  $m$  as given in Lemma 1,

$$P_{[\alpha]}^{(n)} = \sum_{g \in G_{m-1}} \frac{e^{-i\varphi^\alpha([g])}}{|G_{m-1}|} U_g^{\otimes n}, \quad (114)$$

where  $U_g$  is the regular representation. Evaluating Fig. 5 yields

$$\sum_{\{b_j \in G_{M-2}\}_j} \left( \prod_{j=1}^{N_1^{(2)}} \frac{e^{-i\phi_{[b_j]}^{x_{1j}^{(2)}}}}{|G_{M-2}|} \left( \prod_{k=1}^{N_{1j}^{(1)}} \frac{e^{-i\phi_{[a_{jk}]}^{x_{1jk}^{(1)}}}}{|G_{M-1}|} \right) \right) \times \begin{array}{cccccccccc} Z^\alpha & X_{g_{111R}} & X_{g_{112L}} & X_{g_{112R}} & X_{g_{113L}} & X_{g_{113R}} & X_{g_{121L}} & X_{g_{121R}} & X_{g_{122L}} & X_{g_{122R}} \\ \hline U_{b_1} & U_{b_1} & U_{b_1} & U_{b_1} & U_{b_1} & U_{b_1} & U_{b_2} & U_{b_2} & U_{b_2} & U_{b_2} \\ \hline U_{a_{11}} & U_{a_{11}} & U_{a_{12}} & U_{a_{12}} & U_{a_{13}} & U_{a_{13}} & U_{a_{21}} & U_{a_{21}} & U_{a_{22}} & U_{a_{22}} \end{array} \quad (115)$$

Here, we use colors to indicate the origin of each object. We denote by  $b_j$  the group elements obtained from decomposing the measurement outcomes of the second round via Eq. (114), and by  $a_{jk}$  those arising from the measurement outcomes in the first round. Inspecting the graphical object in Eq. (115), we see that the last term is a product of objects of the form

$$\begin{array}{c} \overline{X_{g_{jkL}} \quad X_{g_{jkR}}} \\ | \qquad | \\ U_{b_1} \qquad U_{b_1} \\ | \qquad | \\ U_{a_{jk}} \qquad U_{a_{jk}} \end{array} \quad (116)$$

As  $U_g$  is the regular representation and  $X_g$  is the right-regular representation, we can evaluate this object as

$$\sum_{e, d_{jk}, d_{jk \ominus 1} \in G} \delta[e = b_j a_{jk} d_{jk \ominus 1} g_{1jkL}] \delta[e = b_j a_{jk} d_{jk} g_{1jkR}] |e\rangle\langle e| \otimes |d_{jk \ominus 1}\rangle \otimes |d_{jk}\rangle \otimes |d_{jk}\rangle. \quad (117)$$

Here, we have introduced the notation  $\ominus$  to indicate the previous value of the multi-index (e.g,  $(1, 2) \ominus 1 = (1, 1)$  and  $(2, 1) \ominus 1 = (1, N_{11})$ ). The graphical object in Eq. (115) is a product of (116) terms, with exception of the first term which required additional care. Firstly, according to the above notation, the first term will also contain  $d_{11 \ominus 1}$ . To simplify, we write this as  $d_{11 \ominus 1} = d$ . Secondly, we have a  $Z^{\alpha_1}$  instead of a  $X_g$ . Therefore, we define  $X_{g11L} = 1$  and the  $Z^{\alpha_1}$  will yield the phase  $\chi_{b_1 a_{11} d}^{\alpha_1}$ . Putting this all together, Eq. (115) becomes

$$\sum_{\substack{\{b_j \in G_{M-2}\}_j \\ \{a_{jk} \in G_{M-1}\}_{jk}}} \left( \prod_{j=1}^{N_1^{(2)}} \frac{e^{-i\phi_{[b_j]}^{x_{1j}^{(2)}}}}{|G_{M-2}|} \left( \prod_{k=1}^{N_{1j}^{(1)}} \frac{e^{-i\phi_{[a_{jk}]}^{x_{1jk}^{(1)}}}}{|G_{M-1}|} \right) \right) \sum_{\substack{\{d_{jk} \in G\}_{jk} \\ d, e \in G}} \chi_{b_1 a_{11} d}^{\alpha_1} \left( \prod_{j=1}^{N_1^{(2)}} \prod_{k=1}^{N_{1j}^{(1)}} \delta[e = b_j a_{jk} d_{jk \ominus 1} g_{1jkL}] \delta[e = b_j a_{jk} d_{jk} g_{1jkR}] \right) |d\rangle \langle d_{N_1^{(2)} N_{1, N_1^{(2)}}^{(1)}} | \otimes \bigotimes_{jk} |d_{jk}\rangle. \quad (118)$$

As  $\chi^{\alpha_1}$  is a 1D irrep of  $G$  with kernel  $G_1 \supseteq G_{m \geq 1}$ , we have that  $\chi_{b_1 a_{11} d}^{\alpha_1} = \chi_d^{\alpha_1}$ . Next, note the LHS and first two terms on the RHS of each delta function constraint are identical. Therefore, rearranging terms we get the recursive conditions

$$d_{jk \oplus 1} = d_{jk} g_{1jk}, \quad (119)$$

where we define  $(g_{1jkL})(g_{1jkR})^{-1} = g_{1jk}$ . Therefore, we have

$$d_{jk} = d \left( \prod_{pq=111}^{jk} g_{1pq} \right) \equiv d_{d,1jk}. \quad (120)$$

Note, in a slight abuse of notation,  $d_{d,1jk}$  has  $d$  in its indices to indicate that it is determined by  $d$  (which we are still summing over). Therefore, summing over  $d_{jk}$  and  $e$ , Eq. (118) simplifies to

$$\sum_{\substack{\{b_j \in G_{M-2}\}_j \\ \{a_{jk} \in G_{M-1}\}_{jk}}} \left( \prod_{j=1}^{N_1^{(2)}} \frac{e^{-i\phi_{[b_j]}^{x_{1j}^{(2)}}}}{|G_{M-2}|} \left( \prod_{k=1}^{N_{1j}^{(1)}} \frac{e^{-i\phi_{[a_{jk}]}^{x_{1jk}^{(1)}}}}{|G_{M-1}|} \right) \right) \sum_{\substack{\{d_{jk} \in G\}_{jk} \\ d, e \in G}} \left( \prod_{j=1}^{N_1^{(2)}} \prod_{k=1}^{N_{1j}^{(1)}} \delta[e = b_j a_{jk} d_{d,1jk} g_{1jkR}] \right) Z^{\alpha_1} |d\rangle \langle d| X_{(\prod_{pq} g_{1pq})}^\dagger \otimes \bigotimes_{jk} X_{(\prod_{pq=11}^{jk} g_{1pq})} |d\rangle. \quad (121)$$

Here, the last term contains a GHZ-like contribution (up to quasi-commuting  $X_g$  and  $Z^\alpha$  operators). However, the delta functions still couple the  $d$  variables associated with the GHZ term to the  $b_j$  and  $a_{ij}$  variables, which must be summed over. We can rearrange the remaining delta-functions to obtain

$$\delta \left[ b_j a_{jk} d_{d,1jk} g_{1jkR} = b_{(jk \oplus 1)_1} a_{jk \oplus 1} d_{d,1(jk \oplus 1)} g_{1(jk \oplus 1)R} \right],$$

where  $\oplus$ , in the same spirit as  $\ominus$ , indicates moving to the next multi-index, e.g.,  $(1, 1) \oplus 1 = (1, 2)$ . Now we distinguish two cases, depending on whether  $jk \mapsto jk \oplus 1$  crosses a substring boundary of  $x^{(1)}$ . First, suppose it does not; i.e., assume that  $(jk \oplus 1) = j(k \oplus 1)$ . Thus, Eq. (122) becomes

$$\delta \left[ a_{jk} d_{d,1jk} g_{1jkR} = a_{j(k \oplus 1)} d_{d,1j(k \oplus 1)} g_{1j(k \oplus 1)R} \right] \quad (122)$$

$$= \delta [d_{d,1jk}^{-1} a_{j(k \oplus 1)}^{-1} a_{jk} d_{d,1jk} = g_{1j(k \oplus 1)L} g_{1jkR}^{-1}], \quad (123)$$

where we have used  $d_{d,1(jk \oplus 1)} = d_{d,ijk} g_{1j(k \oplus 1)}$  and  $g_{1j(k \oplus 1)} = g_{1j(k \oplus 1)L} g_{1j(k \oplus 1)R}^{-1}$ . As  $a_{jk} \in G_{M-1} \trianglelefteq G$ , the above condition gives us a constraint that  $g_{1j(k \oplus 1)L} g_{1jkR}^{-1} \in G_{M-1}$ . Moreover, we may eliminate  $d_{d,1jk} \in G$  (which recall, depends on  $d$ ) by noting that as  $a_{jk} \in G_{m-1}$ , it commutes with all elements in  $G$ . Thus, we have

$$\begin{aligned} &= \delta [a_{j(k \oplus 1)} = a_{jk} \tilde{g}_{1jk}] \delta [\tilde{g}_{1jk} \in G_{M-1}] \\ &= \delta \left[ a_{jk} = a_{j1} \left( \prod_{q=1}^k \tilde{g}_{1jq} \right) \right] \delta [\tilde{g}_{1jk} \in G_{M-1}], \end{aligned} \quad (124)$$

for  $k \in \{2, \dots, N_{1j}^{(2)}\}$  where we have defined  $\tilde{g}_{1jk} = g_{1jkR}g_{1j(k\oplus 1)L}^{-1}$ .

We now do the same considering when  $jk \mapsto jk \oplus 1$  crosses a substring boundary of  $x^{(1)}$ , i.e.,  $k = N_{1j}^{(2)}$  and  $(jk \oplus 1) = (j \oplus 1), 1$ . This time Eq. (122) reduces to

$$\begin{aligned} & \delta \left[ b_j a_{jN_{1j}^{(2)}} d_{d,1jN_{1j}^{(2)}} g_{1jN_{1j}^{(2)}R} = b_{j\oplus 1} a_{(j\oplus 1)1} d_{d,1(j\oplus 1)1} g_{1(j\oplus 1)1R} \right] \\ &= \delta \left[ d_{d,1jN_{1j}^{(2)}}^{-1} a_{(j\oplus 1)1}^{-1} b_{j\oplus 1}^{-1} b_j a_{jN_{1j}^{(2)}} d_{d,1jN_{1j}^{(2)}} = g_{1(j\oplus 1)1L} g_{1jN_{1j}^{(2)}R}^{-1} \right]. \end{aligned} \quad (125)$$

Thus, this time we get the constraint  $\tilde{g}_{1(j\oplus 1)1} \in G_{m-2}$ . Moreover, for all  $g \in G$  and  $b \in G_{m-2}$ , there is some  $a_{b,g} \in G_{m-1}$  such that we have  $gb = bga_{b,g}$ . Therefore, rearranging, we have

$$b_{(j\oplus 1)} = b_j \tilde{g}_{1(j\oplus 1)1} \tilde{a}_{d,1jk} \quad (126)$$

$$\begin{aligned} \Rightarrow b_j &= b_1 \left( \prod_{p=1}^j \tilde{g}_{1p1} \right) \tilde{a}_{d,1jk} \\ \Rightarrow [b_j] &= [b_1 \left( \prod_{p=1}^j \tilde{g}_{1p1} \right)], \end{aligned} \quad (127)$$

for some  $\tilde{a}_{d,1jk}, \tilde{a}_{d,1jk} \in G_{M-1}$  which depend on  $j, k$  and  $d$ . Note, however, in taking the quotient map, we lose the dependence on  $d$ . Putting this all together, Eq. (121) becomes

$$\begin{aligned} & \left( \prod_{j \geq 2} \delta[\tilde{g}_{1j1} \in G_{M-2}] \right) \left( \prod_{jk \neq j \geq 2,1} \delta[\tilde{g}_{1jk} \in G_{M-1}] \right) \\ & \left( \prod_{j=1}^{N_1^{(2)}} \frac{e^{-i\phi_{1j}^{(2)}}}{|G_{M-2}|} \left( \prod_{k=1}^{N_1^{(1)}} \frac{e^{-i\phi_{1jk}^{(1)}}}{|G_{M-1}|} \right) \right) \sum_{d \in G} Z^{\alpha_i} |d\rangle \langle d| X_{\left( \prod_{pq} g_{1pq} \right)}^{\dagger} \otimes \bigotimes_{jk} X_{\left( \prod_{pq=11}^{jk} g_{ipq} \right)} |d\rangle. \end{aligned} \quad (128)$$

That is, for each substring,  $x_i^{(2)}$ , we get a segment of the desired GHZ state up to proportionality and quasi-commuting local unitaries.

The same argument holds for the substrings associated with Part 2. The only difference is there is no physical site associated with the (116) terms. In the Part 2 protocol, it is possible to “skip” measurements associated with a given level of the irrep hierarchy (see measurements associated with the first level of the irrep hierarchy in last image of Fig. 4). However, the calculation goes through as before because  $P_{[\alpha]_{m-1}}^{(n)} = P_{[\alpha]_{m-1}}^{(n)} P_{[1]_m}^{(n)}$ , so we can simply insert  $P_{[1]_m}^{(n)}$  wherever a measurement has been “skipped”. Therefore, putting all the substrings together, the final output state is, up to proportionality and quasi-commuting unitaries, a GHZ state.

Finally, we must account for what happens when we require circuits between measurements. In these cases, the delta functions in Eq. (118) become

$$\delta[e = b_{ijk} a_{ijkm} d_{\sigma^{-1}(ikm) \ominus 1} g_{ikmL}] \delta[d_{\sigma^{-1}(ikm) \ominus 1} g_{ikm} = d_{\sigma^{-1}(ikm)}] \quad (129)$$

where  $\sigma$  corresponds to the cumulative permutation implements by the circuits during the protocol. However, all this does is rearrange the arguments of the delta functions and the product of those rearranged delta functions is the same object (e.g.,  $\delta[a = b]\delta[b = c] = \delta[a = c]\delta[c = b]$ ). Thus, the outputted state is still a GHZ state up to quasi-commuting unitaries. Finally, it is clear how the techniques demonstrated in this proof generalize to arbitrary class- $M$  nilpotent groups.

## E GHZ protocol: Probability distribution of measurement outcomes

In this section, we prove that the probability distribution for each measurement outcome during the protocol of Section 6 is uniform, with a probability depending only on the dimension of the corresponding subspace onto which you are projecting. As before, it is sufficient to consider a measurement in round  $m = 3$  having previously measured  $x^{(1)}$  and  $x^{(2)}$ . All other rounds can be derived similarly. Moreover, as before, it is easier

to first consider a sequence of outcomes which happen to require no circuits between measurements and then consider the effect of the circuits at the end. Therefore, we have (compare with Eq.(27))

$$p(\mathbf{x}^{(3)} | \mathbf{x}^{(1)}, \mathbf{x}^{(2)}) = \frac{\text{Diagram 130 Numerator}}{\text{Diagram 130 Denominator}} \quad (130)$$

where the blue boxes correspond to round 1 measurements, green boxes round 2 and orange boxes round 3. As we assume no circuits are required, we can decompose the measurement outcomes of each round in Appendix D, e.g.,  $\mathbf{x}^{(2)} = (\mathbf{x}_i^{(2)})_{i=1}^{N^{(3)}} = ((x_{ij}^{(2)})_{j=1}^{N_i^{(2)}})_{i=1}^{N^{(3)}}$ . Let us consider the left-most measurement from round 3 in the numerator of Eq. (130):

$$\text{Diagram 131: A detailed view of the left-most measurement from round 3. It shows a sequence of operations (blue boxes) followed by a measurement (green box) labeled x_1^{(3)}. Below this, there are multiple sub-measurements labeled x_{11}^{(2)}, ..., x_{1N_1^{(2)}}^{(2)} and x_{111}^{(1)}, ..., x_{1N_1^{(1)}}^{(1)}."/>$$

As before, we use Lemma 1 to evaluate this expression. Again, we will have loops of the form

$$\boxed{\begin{array}{c} U_{c_1} \\ \downarrow \\ U_{b_j} \\ \downarrow \\ U_{a_{jk}} \end{array} \quad \boxed{\begin{array}{c} U_{c_1} \\ \downarrow \\ U_{b_{((jk)\oplus 1)_1}} \\ \downarrow \\ U_{a_{(jk\oplus 1)}} \end{array}}} \quad (132)$$

where, as in Appendix D, the  $\oplus$  notation indicates the next entry in the multi-index, e.g.,  $(1, 1) \oplus 1 = (1, 2)$ , and the subscript picks out the corresponding sublist, e.g.,  $(1, 2)_1 = (1)$ . The physical leg (red line) force this to evaluate as

$$|G| \delta [c_1 b_{ij} a_{ijk} = 1] \delta [c_1 b_{i(jk\oplus 1)_1} a_{i(jk\oplus 1)} = 1], \quad (133)$$

where 1 is the identity element of  $G$ . Note, the second delta function will appear in the next loop. Thus, Eq. (131) can be evaluated as

$$\sum_{\{c_1 \in G_{M-3}\}} \sum_{\{b_{1j} \in G_{M-2}\}_j} \sum_{\{a_{1jk} \in G_{M-1}\}_{jk}} \left( \frac{e^{-i\phi_{[c_1]}^{x_1^{(3)}}}}{|G_{M-3}|} \left( \prod_{j=1}^{N_1^{(2)}} \frac{e^{-i\phi_{[b_{1j}]}^{x_{1j}^{(2)}}}}{|G_{M-2}|} \left( \prod_{k=1}^{N_{1j}^{(1)}} \frac{e^{-i\phi_{[a_{1jk}]}^{x_{1jk}^{(1)}}}}{|G_{M-1}|} \right) \right) \right) \left( \prod_{j=1}^{N_1^{(2)}} \prod_{k=1}^{N_{1j}^{(1)}} |G| \delta [c_1 b_{1j} a_{1jk} = 1] \right) \sum_{d \in G} \langle d | \langle c_1 b_{1N_1^{(2)}} a_{1N_1^{(2)} N_{1N_1^{(2)}}^{(3)}} d | \quad (134)$$

Now consider the delta-functions. The first delta function is only satisfied if  $c_1 = a_{111}^{-1} b_{11}^{-1} \in G_{M-2}$ . Therefore  $[c_1] = [1]$ . Moreover, we must have  $c_1 b_{11} a_{111} = 1 = c_1 b_{1j} a_{1jk}$  for all  $j, k$ . Thus,  $a_{1jk} = a_{1j1}$  and therefore  $[a_{1jk}] = [a_{1j1}]$  for all  $j$  and  $k$ . Moreover,  $b_{1j} = b_{11} a_{111} a_{1j1}^{-1}$  and therefore  $[b_{1j}] = [b_{11}]$  for all  $j$ . As  $\circ_k x_{1jk}^{(1)} = [1]$  and  $\circ_j x_{1j}^{(2)} = [1]$  for all  $j, k$ , Eq. (131) therefore ultimately reduces to

$$\frac{|G_{M-2}|}{|G_{M-3}|} \left( \frac{|G_{M-1}|}{|G_{M-2}|} \right)^{N_1^{(2)}} \left( |G| \frac{|G_M|}{|G_{M-1}|} \right)^{\sum_j N_{1j}^{(1)}} \sum_{d \in G} \langle d d |. \quad (135)$$

Eq. (131) is just the first term in the numerator of Eq. (130), but its clear that the next term will proceed the same way, and so on for each  $i$  up until  $N^{(3)}$ . Moreover, the denominator will also evaluate the same way but without the  $\frac{|G_{M-2}|}{|G_{M-3}|}$  term. Thus the overall probability is given by

$$p(x^{(3)}|x^{(2)}x^{(1)}) = \frac{|G_{M-2}|^{N^{(3)}}}{|G_{M-3}|}. \quad (136)$$

That is,  $p(x^{(3)}|x^{(2)}x^{(1)})$  a uniform multinomial distribution, without any parity constraints. This same argument will hold for all measurement rounds in Part 1. Moreover, because  $P_{[\alpha]_{m-1}}^{(n)} = P_{[\alpha]_{m-1}}^{(n)} P_{[1]_m}^{(n)}$ , it follows that the same holds for the measurements in Part 2. Finally, if there are circuits between rounds, this only introduces a permutation to indices in the delta functions. As the delta functions are linked, the global probability distribution is the same.